63-1-5

ASD-TDR-62-237

NEW APPROACHES TO FLIGHT VEHICLE STRUCTURAL VIBRATION ANALYSIS AND CONTROL

TECHNICAL DOCUMENTARY REPORT NO. ASD TDR 62-237

October 1962

Flight Dynamics Laboratory
Aeronautical Systems Division
Air Force Systems Command
Wright-Patterson Air Force Base, Ohio

Project No. 1370, Task No. 137009

(Prepared under Contract No. AF33(616)-7973
by BOLT, BERANEK AND NEWMAN, INCORPORATED
Cambridge, Massachusetts
Authors: Manfred A. Heckl, Richard H. Lyon,
Gideon Maidanik & Eric E. Ungar)

NOTICES

When Government drawings, specifications, or other data are used for any purpose other than in connection with a definitely related Government procurement operation, the United States Government thereby incurs no responsibility nor any obligation whatsoever; and the fact that the Government may have formulated, furnished, or in any way supplied the said drawings, specifications, or other data, is not to be regarded by implication or otherwise as in any manner licensing the holder or any other person or corporation, or conveying any rights or permission to manufacture, use, or sell any patented invention that may in any way be related thereto.

Qualified requesters may obtain copies of this report from the Armed Services Technical Information Agency, (ASTIA), Arlington Hall Station, Arlington 12, Virginia.

This report has been released to the Office of Technical Services, U.S. Department of Commerce, Washington 25, D.C., in stock quantities for sale to the general public.

Copies of this report should not be returned to the Aeronautical Systems Division unless return is required by security considerations, contractual obligations, or notice on a specific document.

12-269M, 300, 12-4-62

FOREWORD

The research work presented in this report was performed by Bolt, Beranek & Newman, Inc., Cambridge, Massachusetts, for the Flight Dynamics Laboratory, Directorate of Aeromechanics, Deputy Commander/Technology, Aeronautical Systems Division, Wright-Patterson Air Force Base under AF Contract Nr AF33(616)-7973. This research is part of a continuing effort to provide design development information and prediction techniques for structural vibrations and dynamics in flight vehicles which is part of the Air Force Systems Command's Applied Research Program 750A, the Mechanics of Flight. The Project Nr is 1370, "Dynamic Problems in Flight Vehicles" and the Task Nr is 137009, "Methods of Vibration Prediction and Control". Lt. N. A. Wrobel of the Flight Dynamics Laboratory was the Project Engineer.

The studies discussed here were performed during the period of February 1961 to January 1962; the present report constitutes the final effort under the above mentioned contract. The work presented in this report represents a joint effort of the authors, with Dr. E. E. Ungar acting as project supervisor.

The authors gratefully acknowledge the assistance rendered by Dr. I. Dyer, Messrs. C. I. Malme and B. G. Watters, and other members of the staff of Bolt, Beranek & Newman, Inc., as well as the valuable comments and criticisms provided by Dr. O. R. Rogers and Lt. N. Wrobel of ASD.

ABSTRACT

New methods are outlined for dealing with the vibration responses of complex flight vehicle structures to local and to diffuse acoustic excitation. Energy absorption at structural joints and acoustic radiation resistance are shown to be important in establishing levels of these responses. Some experimental results pertaining to energy absorption coefficients and radiation resistance are given, and procedures for estimating the latter are discussed.

Feasibility studies of vibration absorbers utilizing viscoelastic spring elements and distributed mass systems and of vibration isolators composed of viscoelastic leaf springs are summarized. Only the latter are found to possess some practical advantages over conventional systems.

The results of experiments are presented which demonstrate that sound-to-structure coupling may be reduced significantly by the use of beams of special design (See page 28) whose stiffness decreases with increasing frequency. An analytical investigation is summarized which shows that generally damping of only the plates of beam-plate systems may be more desirable than damping of only the beams.

Results of exploratory studies are presented dealing with the mechanisms responsible for the damping of aircraft structural joints, and analytical investigations of the relation between structural joint absorption coefficients and loss factors are summarized. Loss factor data pertaining to two actual aircraft substructures are appended.

PUBLICATION REVIEW

This report has been reviewed and is approved.

FOR THE COMMANDER:

William C. Nielsen

WILLIAM C. NIELSEN
Colonel, USAF
Chief, Flight Dynamics Laboratory

TABLE OF CONTENTS

TABLE OF CONTENTS (Cont)

LIST OF ILLUSTRATIONS

LIST OF ILLUSTRATIONS (Cont)

INTRODUCTION

The increasing abundance of intense sources of broadband vibration associated with present and future air/space vehicles tends to make control of structural vibratory responses essential if structural fatigue failures and equipment malfunctions are to be kept within reasonable limits.

The design engineer has available analytical methods and technological developments that permit him to design simple structures to withstand simple (narrow-band) excitation. However no methods appear available at present that permit him to deal similarly with complicated structures subject to more complex excitation.

The work summarized in this report was undertaken as a step toward providing the lacking design information. Part I of this report outlines studies directed at identifying the parameters that affect the responses of complicated structures most directly: Section IA deals with systems excited at a point. Section IB with systems excited by a diffuse acoustic field. Part II deals with more specific vibration control techniques. Sections IIA and IIC describe feasibility studies of viscoelastic leaf spring isolators and nonclassical vibration absorbers. Section IIB demonstrates the reduction of sound to structure coupling attainable with beams designed to have decreasing flexural rigidity with increasing frequency.* Results of an analytical study related to optimum placement of damping treatments are discussed in Section IID and results of experiments aimed at revealing the salient features of the damping inherent in aircraft structural joints are presented in Section IIE. The final section IIF summarizes initial analytical results pertaining to the relation between structural loss factors and absorption coefficients. Appendix I constitutes a detailed discussion of modal densities: Appendix II summarizes loss factors measured on two substructures of an actual aircraft.

*These beams are the subject of patent applications being filed in the United States and other countries by Bolt, Beranek and Newman, Inc.

Manuscript released by the authors 30 March 1962
for publication as an ASD Technical Documentary Report.

SECTION I

PARAMETERS AFFECTING RESPONSES OF COMPLICATED STRUCTURES

If one attempts to solve in detail the various coupled equations of motion that describe the dynamic behavior of a structure one encounters intractable mathematics for all but the simplest structures. One may therefore wish to sacrifice detail for tractability and search for a method that will permit one to describe in simple terms the average vibration of a complex structure, so that the salient parameters of the structural response may be understood and controlled in design.

A. Point-Excited Structures; Room Acoustics Analogy

In describing the acoustics of a room one faces many of the problems that one encounters also in determining the vibrations of complicated elastic structures. In room acoustics one cannot solve the wave equation in detail because of the complexities of geometry and of the interactions between the waves and the room boundaries. Instead, one recognizes the diffuse character of the sound field and may then calculate some of its average characteristics, based on some average properties of the room and its boundaries.

Similarly, detailed solutions of the equations of motion of structural systems get out of hand very rapidly as the complexity of these systems increases. Therefore one is led to emulate room acoustics, postulate a diffuse wave field in the structure to be studied, and attempt to calculate mean properties of the vibration from relatively rough descriptions of the structure and its boundaries.

The work reported in this section attempts to set down the reasoning as applied to complex structures (composed of beam and plate-like sub-structures), to delineate the important parameters, and to describe some experimental results that validate the theoretically developed relations.

1. Basic Concepts

The energy E with which a structure of total mass M vibrates may be expressed as

$$E = M \overline{v^2} \qquad (A.1)$$

in terms of the mean square velocity $\overline{v^2}$ of the structure, if it is assumed that this energy is uniformly distributed.

If there are mechanisms that remove energy from the structure (as there always are in practical systems) then one must supply energy to the structure in order to maintain a given level of vibration. When the power supply is "turned off", the energy in the structure may be expected to decay. If this decay is assumed to vary as $e^{-\delta t}$, where t denotes time, then the power loss is $-dE/dt=\delta E$. In the steady state the power input P must equal the power loss, so that one may write

$$P = \delta \overline{Mv^2} = \frac{13.8}{T} \overline{Mv^2} \quad . \tag{A.2}$$

The reverberation time $T=13.8/\delta$ introduced here is a quantity that lends itself well to experimental determination; it is defined (ref. 1) as the time required for the energy to decrease by a factor of 10^6.

At frequency f the power loss in the interior of the structure may be described (ref. 2) in terms of the structural loss factor η, as $P_{int}=2\pi f\eta E$. Losses at the boundaries of the structure, on the other hand, may be more conveniently treated in terms of the concept of absorption coefficients. The absorption coefficient of a boundary is defined as the ratio of absorbed power to incident power at that boundary. If a system of waves moving along a structure encounters a boundary, some energy is absorbed, the rest is reflected and propagated until it meets another boundary, etc. The energy absorbed at one encounter with the boundary is γE, where γ denotes the absorption coefficient as defined previously. The number of boundary encounters per unit time may be expressed as c_g/L_m, where c_g denotes the group velocity of the waves on the structure* (the velocity at which energy propagates) and L_m the mean free path (the mean distance travelled by the wave train between boundary encounters). The mean power loss per unit time at the boundaries thus is $P_{bdry}=\gamma E c_g/L_m$, where γ denotes the mean absorption coefficient.

If the boundary is not uniform, γ may be obtained from

$$\gamma L = \Sigma \gamma_i L_i \tag{A.3}$$

where γ_i is the absorption coefficient of the $i^{\underline{th}}$ piece of boundary (which has length L_i), and where $L=\Sigma L_i$ denotes the total boundary circumference. By combining the relations for internal and boundary power losses one may obtain

---

*For a plate of flexural rigidity D and surface density μ, $c_g=2\sqrt{2\pi f}\sqrt[4]{D/\mu}$.

$$P = \delta E = [2\pi f\eta + \gamma c_g/L_m]E \qquad (A.4)$$

Kosten (ref. 3) has shown that for two-dimensional systems the mean free path $L_m=\pi S/L$, where S is the total surface area. Hence the foregoing result may be written as

$$\delta = \frac{13.8}{T} = 2\pi f\eta + \frac{c_g}{\pi S} \Sigma \gamma_i L_i \quad , \qquad (A.5)$$

which is closely related to a result given by Cremer (ref. 4). Eqs. (A.2) and (A.5) contain the salient results of the foregoing discussion. Eq. (A.2) permits calculation of $\overline{v^2}$ from input power, mass M, and reverberation time T (or decay constant δ), and Eq. (A.5) expresses T or δ in terms of internal losses (described by η) and boundary absorption coefficients γ.

The assumptions underlying the foregoing derivations are:

1. Energy uniformly distributed over structure (wave field diffuse; wavelength much smaller than mean free path).

2. Exponential decay of energy with time.

3. Group velocity (not phase velocity) and Kosten's mean free path relation apply.

4. Boundary absorption contributions add linearly (Eq. A.3).

The general validity of these assumptions is by no means self-evident. The results of some experiments, undertaken to verify applicability of these assumptions, are discussed in the following section.

2. Experimental Verification

1) The validity of Eq. (A.2) and of the underlying assumption of uniform energy distribution was verified by measuring the input impedance of a point-driven plate and comparing the measured values to those predicted from relations involving Eq. (A.2) and separately measured reverberation times. Good agreement was obtained over the entire test frequency range.

2) Exponential decay of energy was verified for a number of beam and plate combinations (excited by impacts) by means of a graphic level recorder. This recorder essentially plots log E vs time, so that a straight line record corresponds to exponential decay. Virtually straight lines were obtained in all experiments of this type.

3) Applicability of group velocity and of Kosten's mean free path expression was verified by means of an experiment which provided a boundary portion of unity absorption coefficient; i.e., a means for permitting all incident energy to leave the structure under consideration. A plate was used in these experiments as the primary structure, a second highly damped plate attached to the first over a portion of one of its edges served to provide a boundary with unity absorption. This "known" absorption coefficient was compared with values obtained experimentally and computed from

$$\gamma_i = \frac{13.8\pi S}{c_g L_i}\left(\frac{1}{T_1} - \frac{1}{T_o}\right) . \qquad (A.6)$$

In this relation, which may be obtained from Eq. (A.5), T_o denotes the reverberation time obtained with $\gamma_i=0$ (i.e., before adding absorbing structures at the i^{th} portion of the boundary), and T_1 denotes the reverberation time observed after addition of the absorber extending over L_i. Equation (A.6) is, in fact, useful for the practical evaluation of absorption coefficients in general.

Again, good agreement between measured γ_i and the predicted value of unity was observed, within the limitations of the experiment.

4) The linear additive property of absorption coefficients indicated in Eq. (A.3) was verified by a number of experiments involving plates with boundary absorption provided by various lengths of damping tape and screwed-on beams, variously oriented. The additive property was found to hold for all configurations tested.

3. Results

a) Limits of Validity

The proposed equations should not be applied blindly to all situations. One may readily visualize, for example, that absorbing devices placed near nodal positions of a structure will have little effect on the motions of the structure, whereas the absorbtion of devices located near anti-nodal positions may be greatly enhanced.

In addition, absorbing structures that are small compared to a flexural wavelength on the primary structure may have their absorption decreased because they can not interact effectively with the wave, and/or they may have their absorption increased somewhat due to effects analogous to acoustic diffraction (refs. 5,6).

b) Absorption Coefficients*

i) Summary of Experimental Results

Figures 1 and 2 summarize the results of absorption coefficient measurements on aluminum plates of 1/16 and 1/32 inch thickness, respectively. The various absorbers that were used are also shown schematically in these figures.

In analogy to room acoustics one may assign structural absorbers to three categories:

1) High frequency absorbers, whose absorption coefficient increases with frequency, e.g., damping tapes.

2) Mid-frequency absorbers, whose absorption peak occurs somewhere in the mid-frequency range (say, between 300 and 8000 cps) and is governed by a resonance phenomenon, e.g., bolted-on beams.

3) Low frequency absorbers, whose absorption is highest at low frequencies and decreases to very small values at high frequencies, e.g., parallel beams with dissipative material on the plate between them.

ii) Absorption Mechanisms

The previously summarized experiments were undertaken primarily to demonstrate the absorption coefficient concepts. The mechanisms that contribute to energy absorption need further exploration, but some conclusions may be deduced from data that are available so far. These conclusions are as follows:

Damping tapes - The dissipative action of these tapes is fairly well understood (ref. 2), although additional work is required to interpret available analyses in terms of the desired absorption coefficients. Theory predicts that the damping action of a tape is, as a first approximation, proportional to the ratio of tape foil thickness to plate thickness. Absorption coefficients measured with the same tape on plates of 1/16 and 1/32 inch thickness were found to be in the ratio 1:2 over essentially the entire frequency range; in good agreement with the theoretical prediction.

Beams bolted to plate, with viscous interlayer. - Energy losses here are undoubtedly due to deformation of the interlayer and thus are associated with relative motion between the beam and plate. Absorption peaks may be expected at maxima of this relative motion, i.e., at resonance of the plate portions between screws (since the beam probably deforms and moves much less than the plate).

---

*Some additional details may be found in Reference 7.

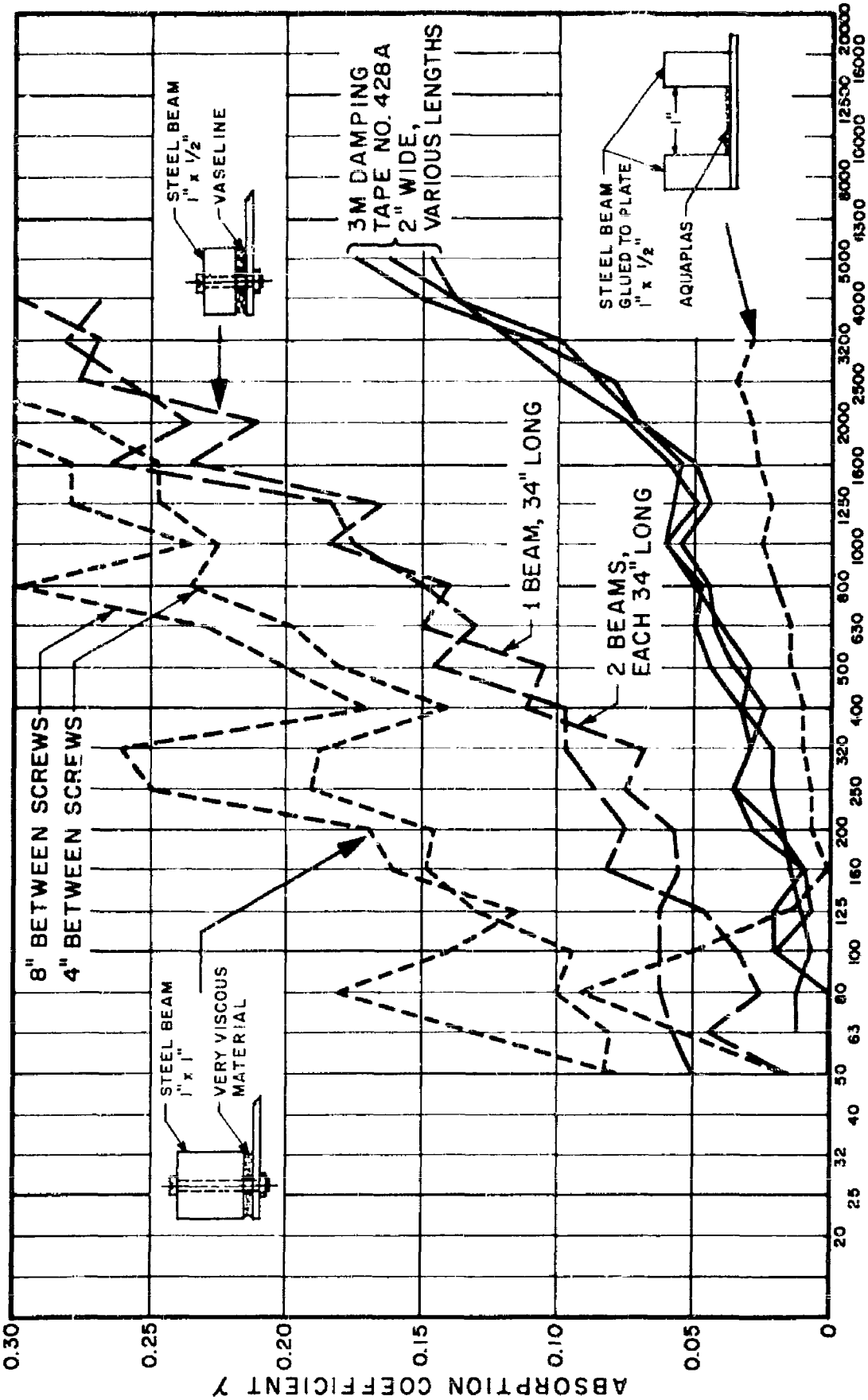

FIG. 1 ABSORPTION COEFFICIENTS MEASURED ON 1/16" THICK ALUMINUM PLATE

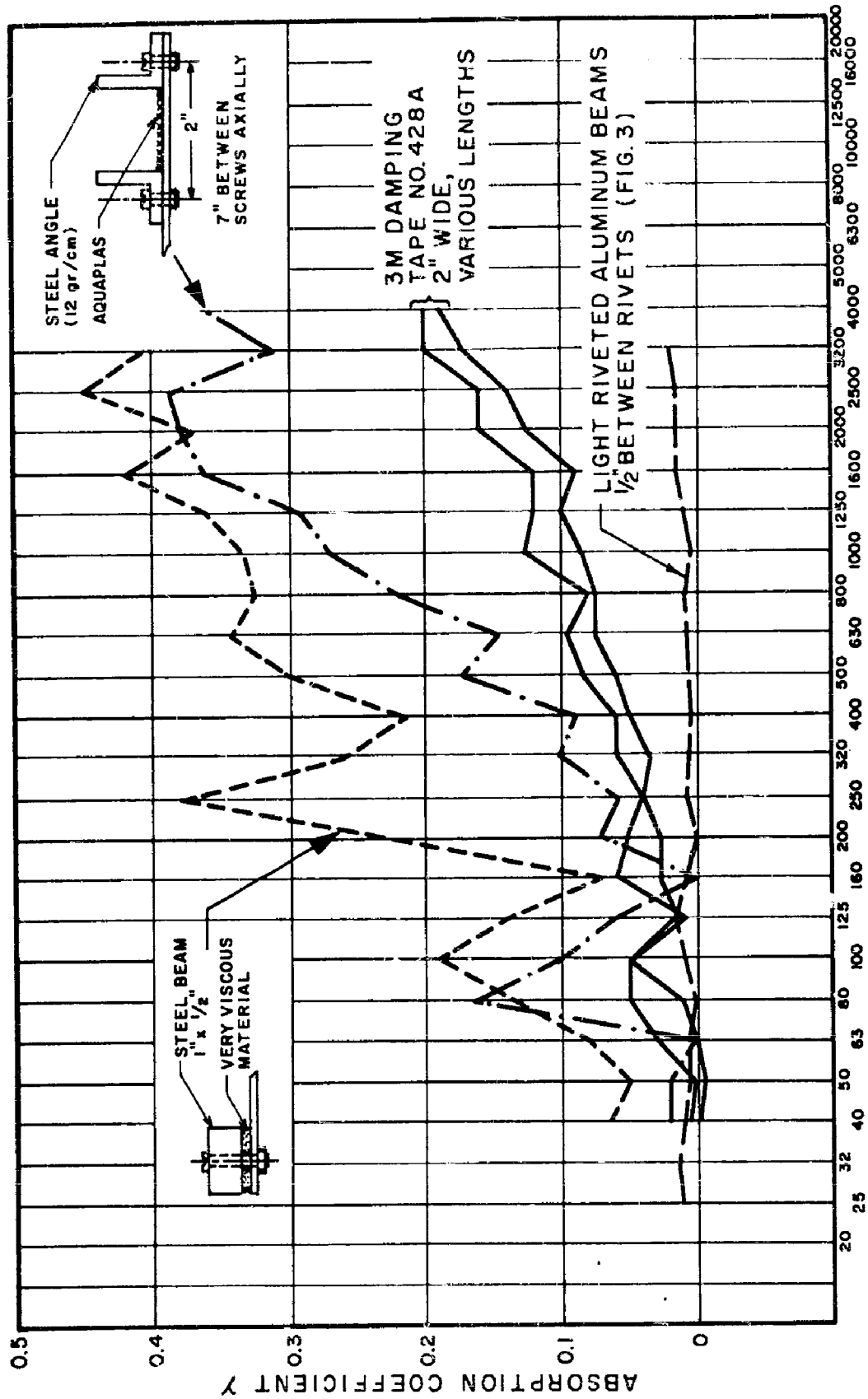

FIG. 2 ABSORPTION COEFFICIENTS MEASURED ON 1/32" THICK ALUMINUM PLATE

It is evident from Fig. 1 that doubling of the distance between screws shifts the first absorption peak by a factor of 4 in frequency, as one would predict on the basis of the aforementioned resonances. The measured values of the first few peak frequencies also agree surprisingly well with values computed as if the plate portions between bolts were simply supported at the bolts. As has been remarked, this type of calculation assumes that the beam acts essentially like an infinitely rigid and massive support for the plate segments. The good agreement observed may be ascribed to the fact that the beams used are very stiff and heavy as compared to the plate; worse agreement should be expected for lighter or softer beams, which may make greater contributions to the relative motion.

Parallel beams, with dissipative material between them - For systems of this type, shown schematically in Figs. 1 and 2, peak absorption may be expected to occur at a resonance frequency determined by the masses of the beams and the spring action of the plate between them. The dissipative mechanism here is provided by deformation of the damping compound (Aquaplas). Frequencies of maximum absorption calculated on this basis agree well with the observed values.

One may observe that at high frequencies the glued-on beams resulted in low absorption (Fig. 1), whereas the bolted-on beams produced fairly high absorption (Fig. 2). This may be due to the glued-on beams' reflecting most of the incident bending wave energy, which thus can not be dissipated by the damping material between the beams. On the other hand, flexural waves which are much shorter than the distance between bolts pass the bolted-on beam virtually unattenuated (ref. 8) and can therefore dissipate much of their energy in the damping material.

Riveted Beams - Measurements indicated in Fig. 2 were performed on a panel made to approximate aircraft construction. This panel is shown in Fig. 3. Absorption here was probably due to friction between the beams and the plates. The low absorption coefficients observed might be due to the close rivet spacing, which restricts the relative motions of beams and plate. See also Section II-E of this report.

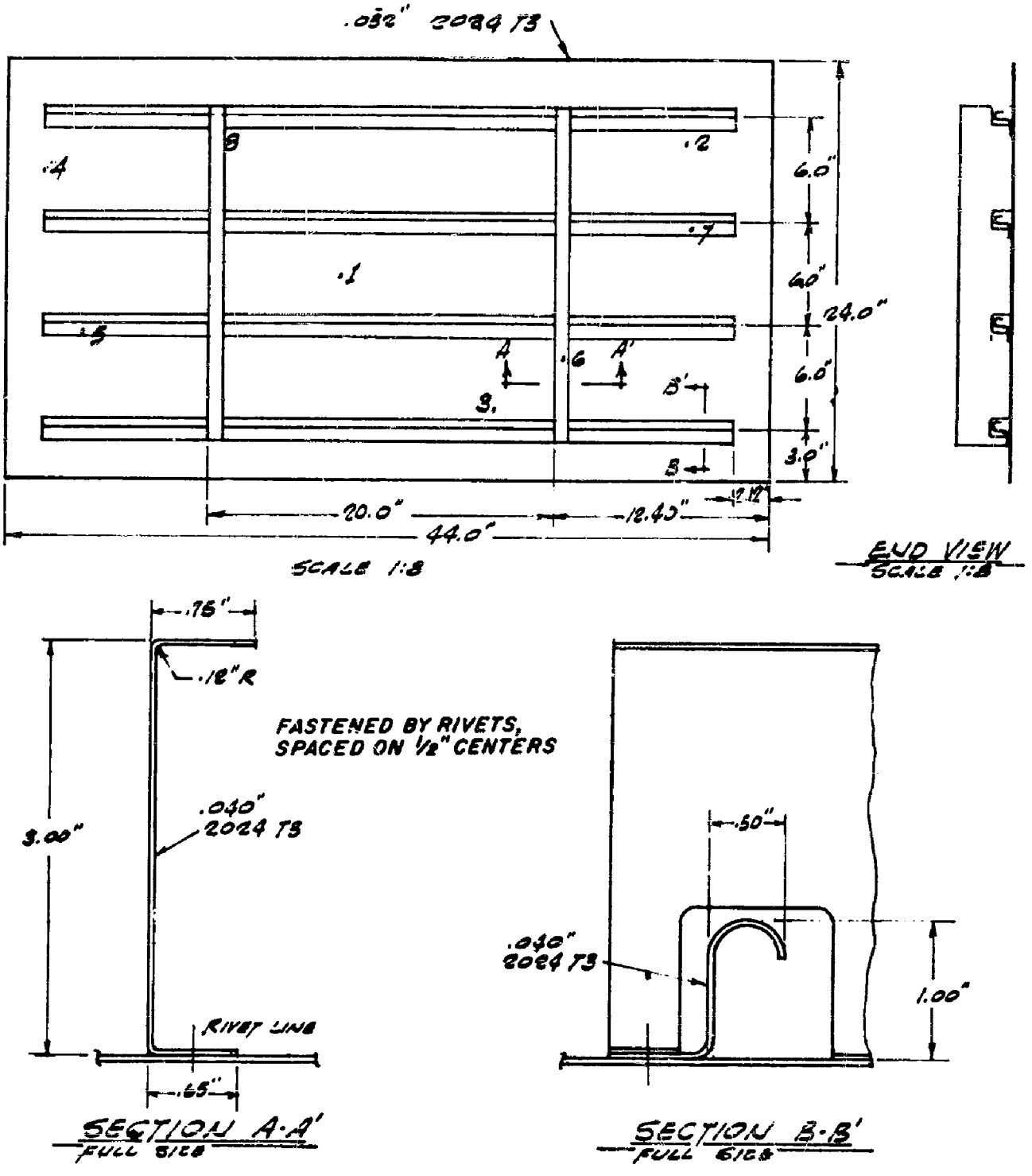

FIG. 3 SIMULATED AIRCRAFT PANEL

B. Structures Excited By Reverberant Acoustic Fields; Application of Energy Concepts

Thermodynamic or energy concepts are generally useful for arriving at some understanding of complex systems, since these concepts do not rely on detailed analyses of the systems involved. These concepts, properly interpreted, might therefore be used to advantage in analyzing the vibrations of complex structures exposed to random acoustic fields.

The average energy associated with a given mode of a structure or of a reverberant room may, in analogy to gas dynamics, be taken as a measure of the "acoustic temperature" of the structure or room in a small frequency interval enclosing the modal frequency. One may then conceive of a reverberant room as a thermal bath in which the structure is immersed and with which it will eventually come to thermal equilibrium. The equilibrium temperature of the structure then depends on the temperature of the room and on how good the thermal contact between the two is. This thermal analogy has been useful in guiding the analyses presented subsequently, but further elaboration on it will be omitted here since it is not essential for summary and application of the results of these studies and since it is available in detail in reference 9.

1. Basic Concepts

a) Modal Behavior

Whenever structural resonances occur in separate sharply defined frequency regions; i.e., whenever the effective structural damping is very small (or the quality factor Q is very high), the various structural modes may be considered as incoherent harmonic oscillators. That is, each mode has associated with it its own modal velocity energy, mass, force, etc.

In complete analogy to relations developed for a single-degree-of-freedom system subject to random excitation, one may express the mean square modal velocity $\overline{v^2}$ as

$$\overline{v^2} = \frac{\pi}{2} \frac{S_f(\omega_o)}{M R_T} \qquad \text{(B.1)}$$

where $S_f(\omega)$ denotes the power spectral density of the modal force f, ω_o the natural frequency associated with the mode, R_T the total resistance (analogous to the usual viscous damping coefficient), and M the modal mass (refs. 10-12).

For structures immersed in acoustic media it is convenient to consider the total resistance as the sum of two terms: one (R_{rad}) to account for energy radiated to the medium, and the other (R_{mech}) to account for other energy losses, such as those due to material hysteresis or "mechanical" damping.

From the work of Smith (ref. 10) one may show that for a structure exposed to a reverberant acoustic field with power spectral density of pressure $S_p(\omega)$, the previously defined S_f is given by

$$S_f(\omega_o) = \frac{4\pi\, c_a}{\rho_a\, \omega_o^2} R_{rad}\, S_p(\omega_o) \quad . \tag{B.2}$$

Here ρ_a denotes the density of the acoustic medium, c_a the speed of sound in it.

By combining Eqs. (B.1) and (B.2) one may obtain the following cogent expression:

$$\theta_S = \theta_R \cdot \mu \tag{B.3}$$

where

$$\theta_S = M\,\overline{v^2} \quad = \text{average energy per structural mode} \tag{B.4}$$

$$\theta_R = \frac{2\pi^2\, c_a}{\rho_a\, \omega^2} S_p(\omega) \quad = \text{average energy per acoustic mode*} \tag{B.5}$$

---

*The total acoustic energy in a reverberant room of volume V in a frequency interval $\Delta\omega$, within which the mean square pressure is $\overline{p^2} = S_p(\omega_o)\cdot\Delta\omega$, is given by

$$E_R = \overline{p^2} V/\rho_a c_a^2$$

and the number of modes in the room in this frequency interval is (ref. 5)

$$N_R = \omega_o^2 V\, \Delta\omega/2\pi^2\, c_a^3 \quad .$$

Hence $\theta_R = E_R/N_R$ is given in Eq. (B.5).

$$\mu = \frac{R_{rad}}{R_{rad}+R_{mech}} = \text{a factor that denotes the degree of coupling between room and structural mode.} \qquad (B.6)$$

Thus, if the various terms that enter Eq. (B.3) are in hand one may utilize this equation to estimate the response of structures to reverberant excitation under the conditions where the assumptions underlying the derivation of Eq. (B.3) are reasonably well satisfied. The remainder of this section will therefore be concerned primarily with evaluation of the various parameters.

b) Parameter Estimates

i) Modal Mass

The modal mass M is defined so that $M\overline{v^2}/2$ gives the average kinetic energy of the structure. The modal mass is between 1/2 and 1 times the total mass, it is nearer 1/2 of the total mass for higher modes.

ii) Coupling Factor μ

It is evident from Eq. (B.6) that for those cases where mechanical damping R_{mech} is much smaller than radiation damping R_{rad}, $\mu \approx 1$. For most practical cases, however, $R_{rad} \ll R_{mech}$, and

$$\mu \approx \frac{R_{rad}}{R_{mech}} \qquad (B.7)$$

Equation (B.3) applies when an acoustic field excites the structure. For the case where the structure excites the acoustic field one finds from a relatively detailed examination of the interaction at $\theta_R = \theta_S$ $\mu' = \mu$ with $\mu' = \mu$.

iii) Mechanical Resistance R_{mech}

As for a simple harmonic oscillator, the average power loss for a mode is $P = R_{\eta}\overline{v^2}$ and the average energy is $E = M\overline{v^2}$. By equating P/E obtained here to the same ratio computed from Eq. (A.4) and noting that generally $R_{mech} \gg R_{rad}$ one may express the mechanical resistance directly in terms of the previously introduced structural loss factor η and absorption coefficient γ:

$$R_{mech} \approx M\left[2\pi f\eta + \frac{Lc}{\pi s}\gamma\right] . \qquad (B.8)$$

If boundary losses predominate over internal losses, as often is the case, then

$$R_{mech} \approx \frac{c_g}{\pi} \frac{M}{S} \Sigma \gamma_i L_i \quad , \tag{B.9}$$

where γ_i is the absorption coefficient of a portion of the boundary of length L_i and $M/S \approx \rho_S/2$ (i.e., M/S is approximately equal to one half the structural mass per unit surface area).

iv) Radiation Resistance R_{rad}

The coincidence phenomenon is known to be a major factor in determining the radiation resistance of simple structures. At frequencies below the coincidence frequency the length of a flexural wave in a structure is greater than the acoustic wavelength in the surrounding medium, and the coupling between the structure and the medium is poor; R_{rad} is small. At frequencies above coincidence the flexural wavelengths are smaller than the acoustic wavelengths, coupling is better, and R_{rad} is greater.

For uniform beams or plates the coincidence frequency f_c is given by

$$2\pi f_c = \omega_c \approx c_a^2/\kappa c_L \quad , \tag{B.10}$$

where κ denotes the radius of gyration of the cross-section ($\kappa = h/\sqrt{12}$ for plates of thickness h), c_a denotes the speed of sound waves in the acoustic medium, and c_L the speed of longitudinal waves in the structural material. Stiffer structural members thus have lower coincidence frequencies and might be expected to exhibit higher average radiation resistances in a given wide frequency band.

In a structure composed of many beams and panels (e.g., a typical aircraft section) one may generally expect to find that some components of the structure are below and others above coincidence at a given frequency. In order to obtain a first approximation to the radiation resistance of such a composite structure one might neglect interaction effects and assume that only those components which are above coincidence contribute significantly to the radiation resistance. Radiation resistance estimation procedures based on these assumptions are outlined below.

Since the beams in most practical beam-plate structures are much stiffer than the plates, the beams should dominate the radiation resistance of such structures at the lower frequencies. The panels, by virtue of their higher coincidence frequencies, may have little effect except at the highest frequencies.

The acoustic radiation of beam-plate systems in which the plates are limp (i.e., soft and damped) may thus be assumed to be primarily due to the beams acting as strip radiators, with the panels acting essentially as baffles, but perhaps adding a little to the width of the strip radiators - in analogy to a similar situation encountered in studies of sound transmission through walls with studs (ref. 13).

The radiation resistance of a strip radiator of length L and width w is (for both faces) given by (ref. 14)

$$R_{strip} = \omega w^2 L \rho_a \quad , \text{ for } \omega > \omega_c \tag{B.11}$$

provided that the strip width w is small compared to the acoustic wavelength. Below coincidence (that is, for $\omega<\omega_c$) the radiation resistance of a strip is much smaller than that given above.

Heckl (ref. 15) has suggested that a strip radiator attached to a limp plates has an effective radiating width $w\approx\lambda_p/\pi$, where λ_p is the wavelength of plate flexural waves. For homogeneous plates,

$$\lambda_p = 2\pi \kappa c_L/\omega \tag{B.12}$$

so that for a beam attached to limp panels,

$$R_{strip} \approx 4L\rho_a \kappa c_L \tag{B.13}$$

where κ and c_L refer to <u>plate</u> radius of gyration and longitudinal wave velocity.

One may note that λ_p decreases with increasing frequency and that R_{strip} is independent of frequency. However, the effective strip width associated with a practical beam probably will not be less than the width of the beam flange in contact with the plate. If this flange width is denoted by w_o, then $\lambda_p/\pi=w_o$ at a frequency f_r given by

$$f_r = \frac{2\kappa c_L}{\pi w_o^2} \quad . \tag{B.14}$$

For $f>f_r$ the radiation resistance of the strip should obey

$$R_{strip} \approx \omega L \rho_a \cdot w_o^2 \quad , \quad f>f_r \tag{B.15}$$

instead of Eq. (B.13).

For a beam-plate structure in which the plates are below coincidence the radiation resistance at frequency f may then be approximated by

$$R_{rad}(f) \approx 4\rho_a \kappa c_L \sum L_{f_c<f<f_r} + 2\pi f \rho_a \sum \left(w_o^2 L\right)_{f>f_r>f_c} \qquad (B.16)$$

where the first summation denotes the total length of beams that at frequency f are above coincidence but below f_r, and the second summation is taken over all beams for which $f>f_r$.

On the other hand, at frequencies which are above the coincidence frequency of the panels, one may expect the radiation to be dominated by that due to the panel. Then, if one neglects edge effects (ref. 1) and takes into account radiation from both faces, where A is the total area of the panels (one face) that are above coincidence,

$$R_{rad} \approx 2A\rho_a c_a \quad , \qquad (B.17)$$

It must be pointed out that in computing radiated power from the defining relation $P=R_{rad}\, v^2$ one must always use that v^2 which refers to the velocity of the radiating section. Since it is the panel that radiates, its velocity must be used in the foregoing expression. (When the panel is "limp" the velocity of that portion of it that is radiation is essentially that of the beam. Validity of the panel velocity under this condition has been demonstrated experimentally, as discussed in the next section.)

A relation between panel velocity v_p and beam velocity v_b may be deduced for the condition of modal independence from the assumption that the average energy per mode is the same for all structural components. Then the energy contributed by a component is proportional to its modal density, and if the beams and the plate are of the same material,

$$\frac{M_b}{M_p}\frac{\overline{v_b^2}}{\overline{v_p^2}} \approx \frac{\kappa_p}{\kappa_b} \quad , \qquad (B.18)$$

where M_p denotes the total panel mass, M_b the total beam mass, and κ_p denotes the plate radius of gyration, κ_b the beam radius of gyration. (This equation assumes the grillage composed of the beams to behave like an equivalent plate (ref. 16). The stiffest beams will influence this behavior most, therefore their κ_p values should be used in this approximate computation.) If beams and plates are of different materials, the right-hand side of Eq. (B.18) should be multiplied by c_{L_p}/c_{L_b}.

It should be remembered that the foregoing procedure for estimating radiation resistance constitutes only of a first step, and as such may be unreliable. Pertinent results of a later study (ref. 17) are discussed under the heading of Conclusions at the end of this section (page 22).

c) Non-Modal Behavior

i) Limit of Modal Behavior

The entire previous discussion is based on the assumption that the structural modes do not overlap in frequency, so that their vibrations are statistically independent and their energies do not interact. Overlap occurs if the frequency bandwidth associated with a mode is of the same order of magnitude as the average frequency separation between modes.

As shown in Appendix I, the plate-like portions of beam-plate systems contribute many more modes than the beam-like portions, so that the former predominate in establishing the separation between modes. The average frequency separation Δf between modes of a panel of area A and thickness h is given by

$$\Delta f \approx hc_L/A\sqrt{3} \quad , \tag{B.19}$$

where c_L denotes the longitudinal wave velocity in the panel material. The same expression applies also for the higher frequencies of a beam-plate system in which all panels are of the same thickness and material; A then denotes the total panel area.

If one assumes for the sake of simplicity that the location of structural modes along a frequency axis may be described by a Poisson process (ref. 18), one may show that the probability of finding more than one mode in a frequency interval Δb is 0.5 or greater if $\Delta b/\Delta f \geq 1.68$. One may then define a "frequency of modal overlap" f_∞ for a structure as that frequency for which the modal bandwidth equals 1.68 Δf. Since bandwidth is related to quality factor Q or loss factor η as $\Delta b = f/Q = \eta f$, the frequency of modal overlap is given by

$$f_\infty = 1.68Q\Delta f = 1.68\,\frac{\Delta f}{\eta} \tag{B.20}$$

At frequencies above this frequency the probability of finding more than one modal peak within bandwidth Δb of a modal response is greater than 0.5. Thus, modal behavior of the structure may reasonably be assumed at frequencies below f_∞.

ii) Estimation of Non-Modal Response

At frequencies above f_∞ a beam-plate structure may be expected to respond to an acoustic field essentially like an infinite plate, and to obey the "mass law" relation

$$S_a(\omega) = 4S_p(\omega)/\rho_S^2 \qquad (B.21)$$

where S_a is the power spectral density of acceleration of the structure, ρ_S is its mean mass per unit surface area.

2. Experimental Results

A series of experiments was undertaken in order to obtain an indication of the validity of the previously outlined theories. These experiments were performed primarily on a simulated aircraft panel (shown in Fig. 3) suspended in a large test room. In each case the experiments were performed with the panel in its original condition and also with some damping (several randomly oriented strips of MMM damping tape) added. All experiments were performed with narrow band noise excitation.

Figure 4 summarizes results obtained from experiments consisting of driving the panel at various points by means of a mechanical shaker and measuring the power P_{rad} radiated to the room as well as the velocity of one point on the panel. (A point on a rib was selected since it was found that the transducer distorted the behavior of the panel at higher frequency when attached to the panel itself.) The measured quantities are interpreted in the figure in terms of radiation resistance R_{rad} according to the relation $P_{rad}=R_{rad}/v_b^2$. The subscript b here indicates that velocity was measured on a beam, rather than on a panel, as previously indicated.

The results of reverberation time measurements on the panel of Fig. 3 are summarized in Fig. 5, interpreted in terms of total resistance $R_T=R_{mech}+R_{rad}$ according to 13.8M/T with the modal mass M taken as 1/2 the total mass.

The upper series of points shown in Fig. 6 represent values of the coupling factor μ' computed according to Eq. (B.6) from the data of Figs. 4 and 5. These points pertain to the case where the panel is driven mechanically and excites acoustic oscillations in the test room. The lower series of points shown in Fig. 6 represents values of the coupling factor μ obtained from additional measurements in which sound in the room excited vibrations in the panel. The latter results were computed on the basis of modal energies, using Eqs. (B.3) and (B.5).

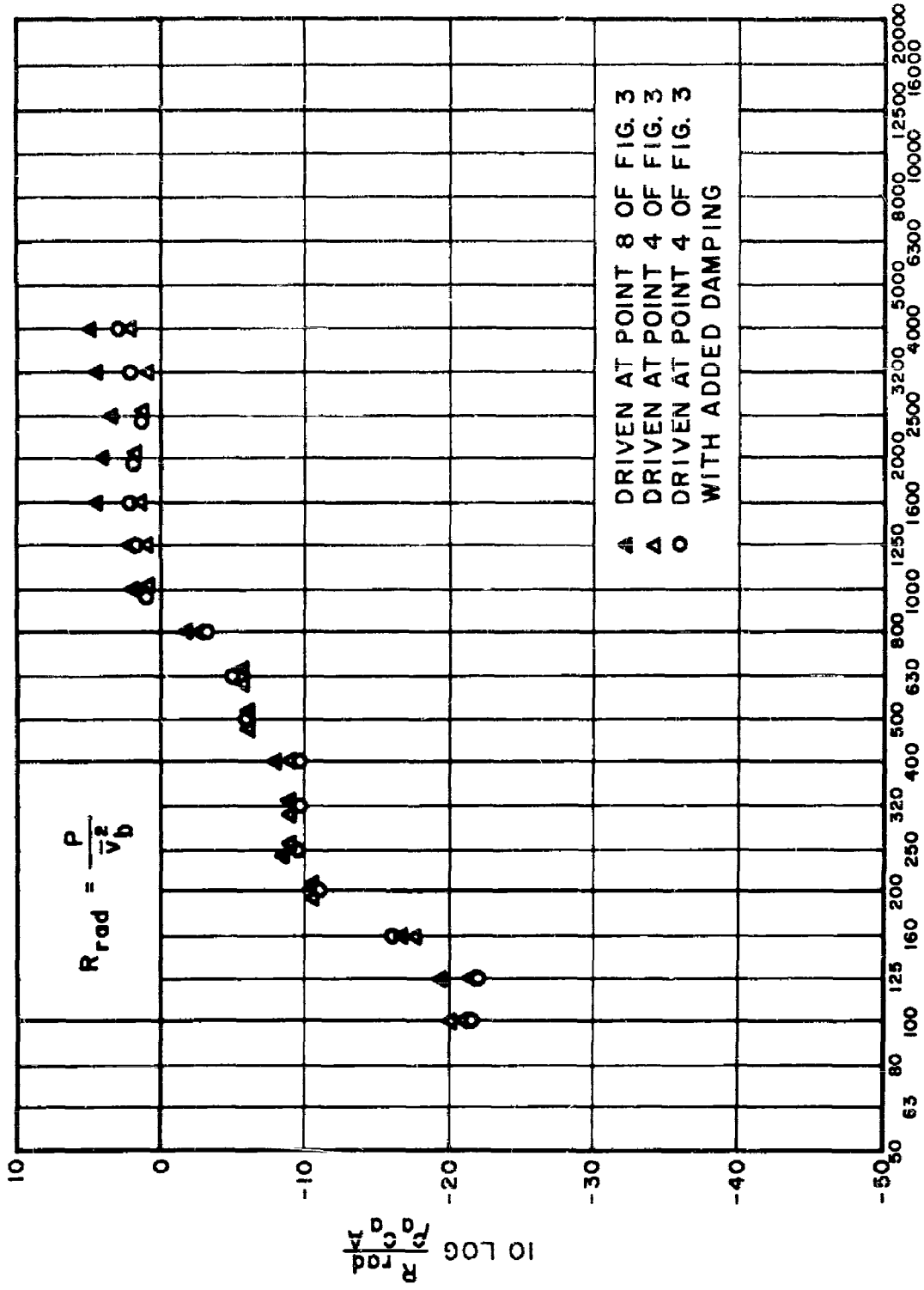

FIG. 4 RADIATION RESISTANCE OF SIMULATED AIRCRAFT PANEL, AS DETERMINED FROM MEASUREMENTS OF POWER RADIATED TO ROOM AND VELOCITY OF POINT 6 OF FIG. 3

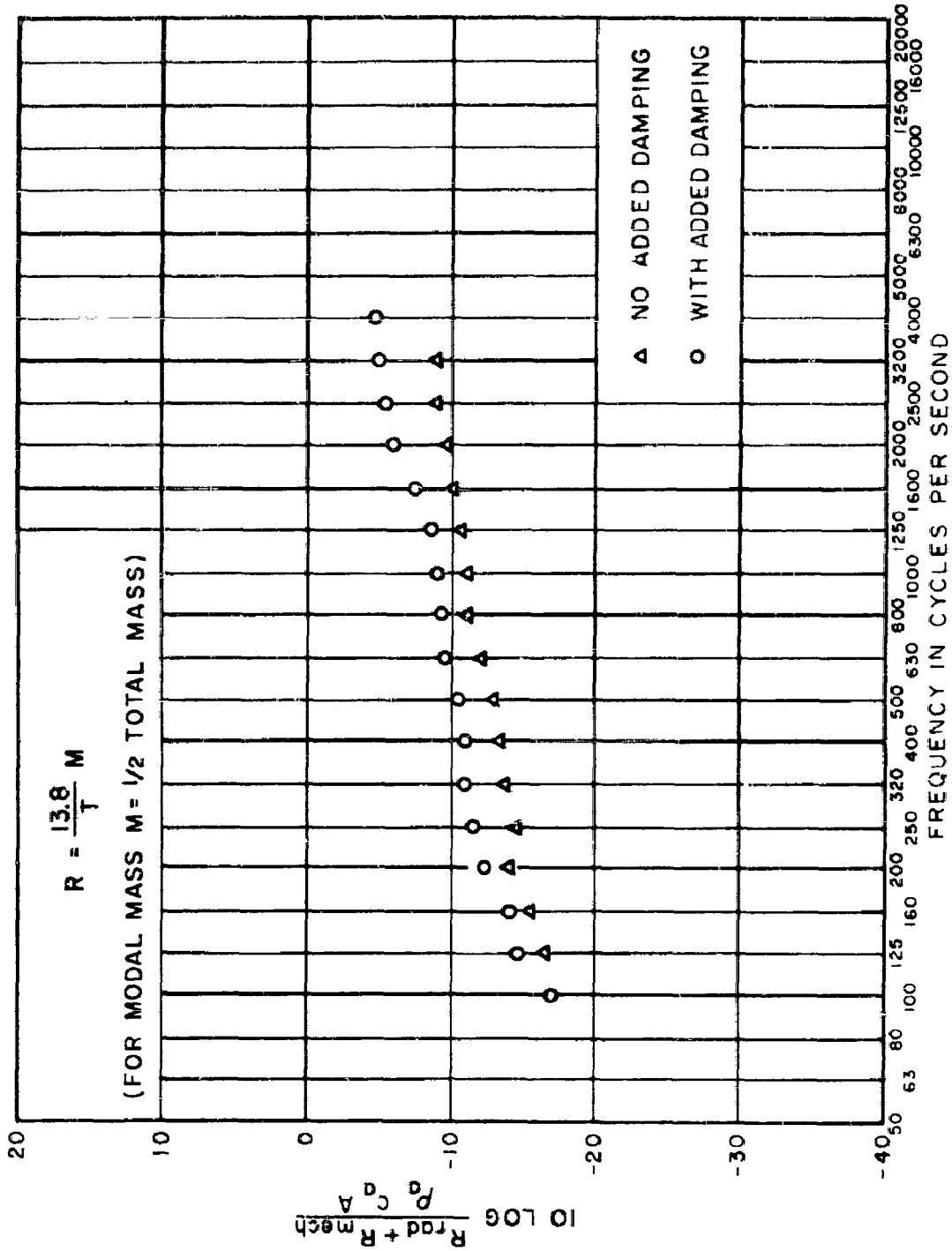

FIG. 5 TOTAL RESISTANCE OF SIMULATED AIRCRAFT PANEL, AS DETERMINED FROM REVERBERATION TIME MEASUREMENTS

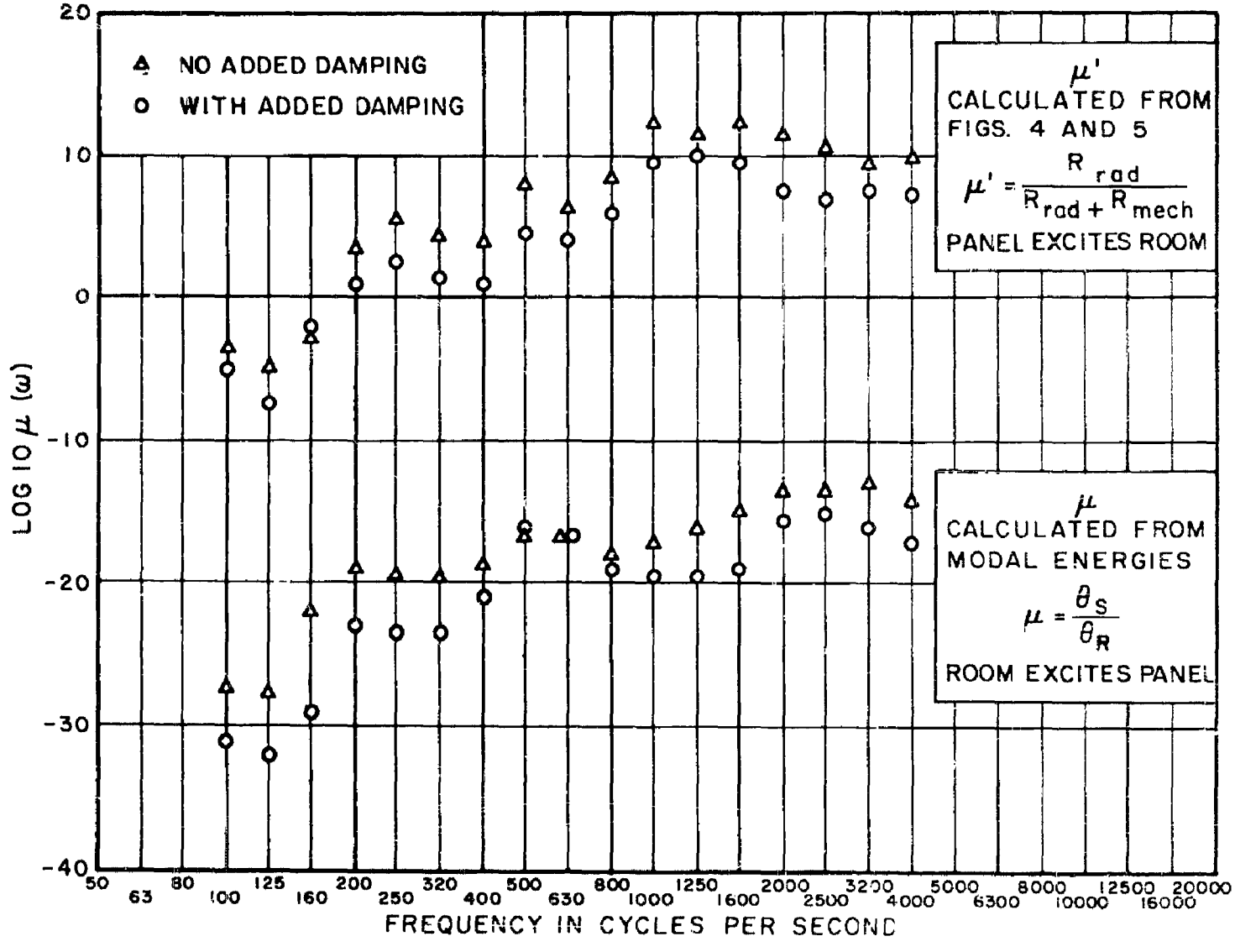

FIG. 6 COUPLING FACTORS μ AND μ' FOR SIMULATED AIRCRAFT PANEL (v_b MEASURED AT PT.6 USED FOR PANEL VELOCITY)

All computations for Fig. 6 were based on the assumption that v_b, as measured at point 6 shown in Fig. 3, represents the velocity of the simulated aircraft panel. Theory indicates that μ and μ' of Fig. 6 should be equal, and it appears that panel velocity v_p instead of beam velocity v_b should be used in the various computations. The radiation resistance $R_{rad}^{(b)}$ referred to a beam is related to that referred to a plate $R_{rad}^{(p)}$ according to

$$P = R_{rad}^{(b)} v_b^2 = R_{rad}^{(p)} v_p^2 \quad . \tag{B.22}$$

Therefore the μ' data of Fig. 6 appears to be too high by a factor of $\overline{v_p^2}/v_b^2$ and the μ data appear to be too low by the same factor. Hence this factor may be computed by comparison of the two sets of data. The results of such a computation are shown in Fig. 7, together with the value estimated from Eq. (B.18) which is based on the assumption of equipartition of energy among all structural modes.

Figure 8 shows the data of Fig. 4 corrected from $R_{rad}^{(b)}$ to $R_{rad}^{(p)}$ by use of the velocity ratio plotted in Fig. 7. Also shown in Fig. 8 are the radiation resistance values predicted by Eq. (B.16).

3. Conclusions

From the foregoing experimental results, and from addition results obtained under NASA sponsorship (ref. 17) subsequent to completion of the work described here, one may arrive at the following conclusions:

1. Equipartition of energy among the structural modes is reasonable and provides a useful estimate of the beam/plate velocity ratio.

2. The modal energy expressions of Eqs. (B.4) and (B.5) appear to be valid, and the modal mass may reasonably be approximated by 1/2 the total mass.

3. Velocity and radiation resistance should be referred to the plate, not to ribs, in calculation of coupling factor μ.

4. Reciprocity holds; i.e., μ' (room driving plate) = μ (plate driving room).

5. Radiation resistance values estimated from Eq. (B.16) always exceed the actual values, occasionally by considerable amounts.

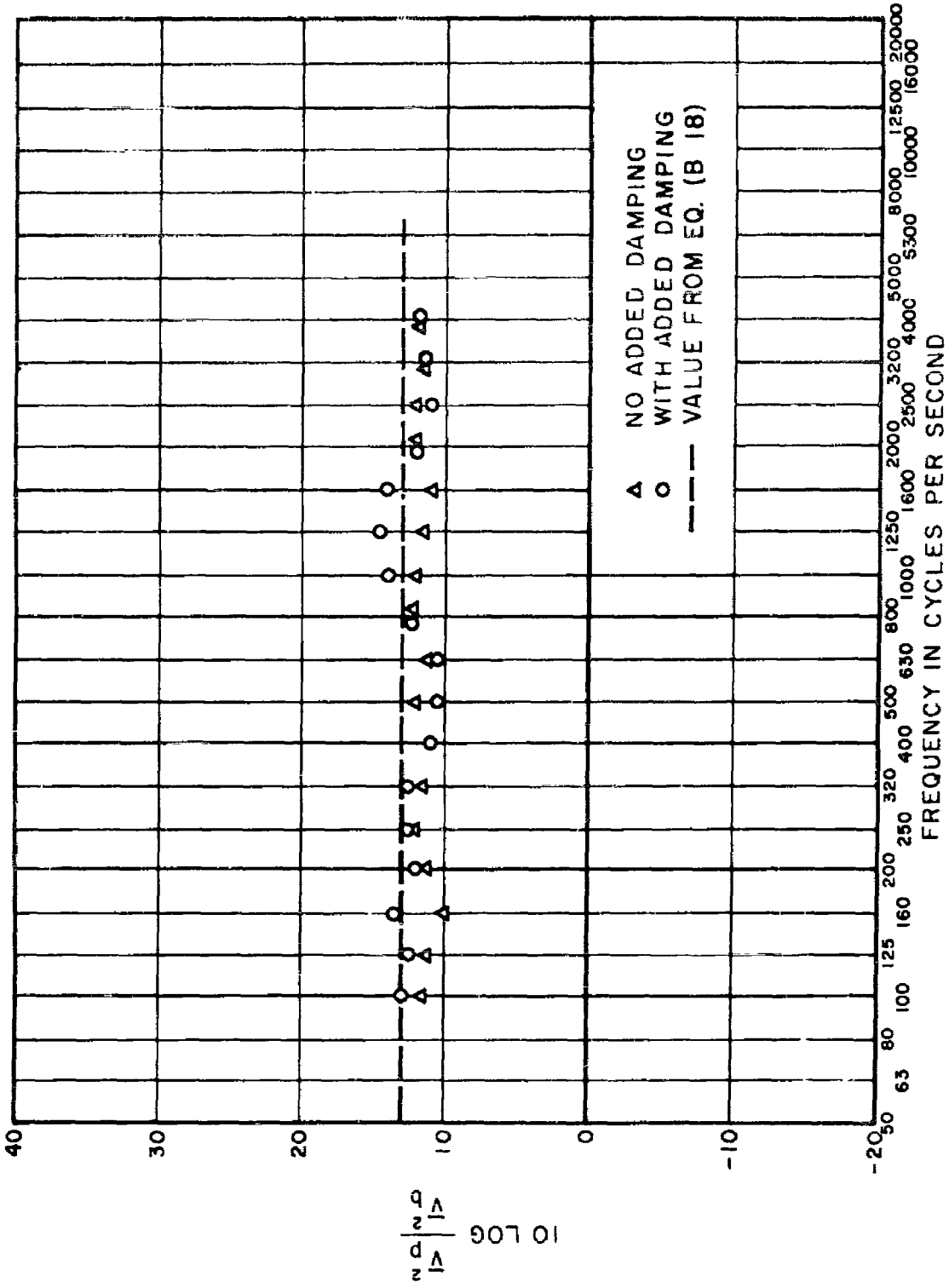

FIG. 7 RATIO OF MEAN SQUARE VELOCITIES OF PANELS AND BEAMS REQUIRED TO MAKE DATA OF FIG. 6 SATISFY RECIPROCITY ($\mu = \mu'$)

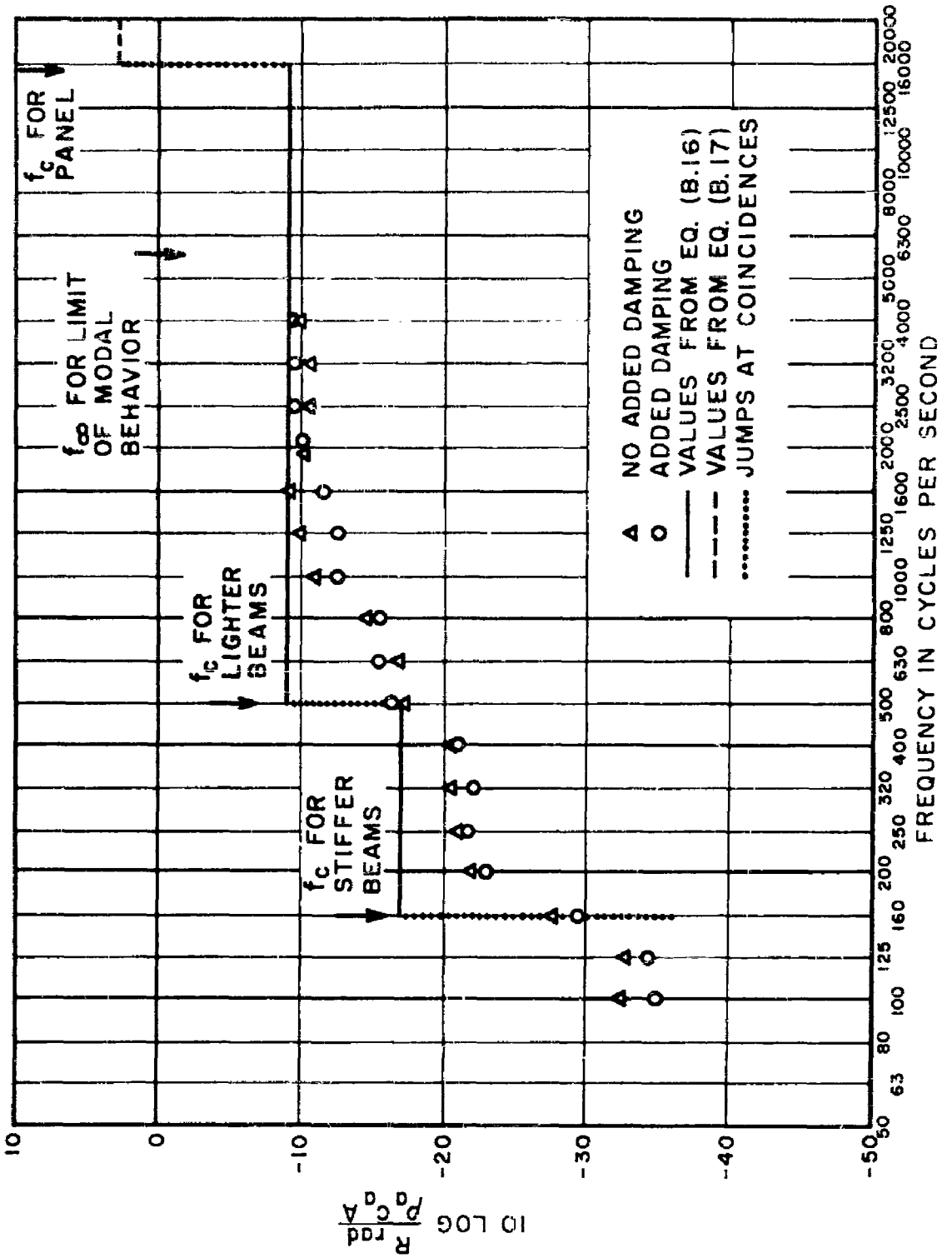

FIG. 8 RADIATION RESISTANCE VALUES OF FIG. 4, CORRECTED FOR PANEL/BEAM VELOCITY RATIO OF FIG. 7

The deviations of experimentally determined from theoretically predicted results apparent in Fig. 8, and more pronounced deviations observed in a later study (ref. 17) performed with a larger and thicker baffled plate with more massive beams, have shed some doubt in the general applicability of the strip radiator concept as outlined here. A later (so far only partially validated) theory (ref. 17) ascribes the radiation resistance of beam-plate structures to the scattering of plate flexural waves at beams, edges, or other discontinuities. The presence of beams, etc., thus is still held responsible for increasing the radiation resistance of the composite structure, but beam coincidences now assume much less importance. The newer model predicts radiation resistance increases due to beam coincidences to be noticeable only with beams that are very light relative to the plate and to occur at frequencies which may be considerably higher than the classical coincidence frequencies of the beams. However, since the strip radiator theory proposed in the present report may be shown on the basis of the newer theory always to result in high estimates of the radiation resistance, the simpler strip radiator theory may still be useful for conservative design estimates.

SECTION II

SPECIFIC VIBRATION CONTROL TECHNIQUES

The maximum responses of structures to vibratory excitation are affected primarily by the magnitude of the excitation, its coupling to the structure, and by the resonant and damping characteristics of the structure. Control of vibration must therefore be concerned with favorable adjustment of these factors.

The structural designer cannot usually hope to do much about controlling the magnitudes of excitation caused by aerodynamic or acoustic phenomena. However, when the excitation is a local one, as for example due to a vibrating machine (that cannot be modified itself), the designer may turn to vibration absorbers to reduce the excitation that reaches the structure. Attempts at devising vibration absorbers with improved characteristics are summarized in the first of the following sections.

Means for reducing the coupling between sources of excitation and structures are discussed in the next two sections. Section B outlines experimental results that demonstrate the utility of "velocity-controlled" beams (whose stiffness decreases with increasing frequency) in reducing the radiation resistance of beam-plate structures. Section C summarizes results of a mathematical study of viscoelastic leaf spring isolators, which may possess some attractive features for reducing the coupling between local sources and structures.

The final three sections deal with aspects of structural damping, which is most important in limiting structural responses. Section D outlines a theoretical study of the interaction of beams and plates in beam-plate systems, in order to determine how application of damping to one or the other of these components affects the system responses. Section E presents the results of a primarily experimental investigation intended as a first step toward understanding and improving the damping of aircraft structural joints. Finally, section F summarizes the derivations of some expressions that relate the loss-factors of beam-like structures to absorption coefficients exhibited by these structures attached to plates.

A. Non-classical Vibration Absorbers

It is well known that one may reduce the steady-state response of a primary mass M to sinusoidal excitation at frequency ω_o by connecting M to a secondary mass m via a spring of stiffness k, so that $\omega_o^2 = k/m$. However, the secondary mass and spring can reduce (i.e., "absorb") the vibration of the primary mass only for frequencies near ω_o. For example,

for driving frequencies only slightly greater than ω_o the "absorber" results in large amplification of the response of M.

1) Frequency-Variable Springs

If the frequency of absorption $\omega_o = \sqrt{k/m}$ could be made to change with driving frequency ω so as to remain equal or nearly equal to it, the resulting device would act like an ideal absorber over the entire range over which this equality is maintained.

Continuous reduction of the secondary mass with increasing frequency appears impossible to obtain practically. However, viscoelastic springs are known to increase in stiffness with increasing frequency. Detailed consideration of the absorber action of viscoelastic springs and of representative suitable materials showed that:

1) The stiffnesses of viscoelastic materials increase at most as the first power of frequency, whereas increase as the square is required for continuous optimum absorption.

2) The most rapid increases of viscoelastic material stiffness occur in conjunction with high damping, which decreases absorber effectiveness.

3) Large ratios of secondary to primary mass would be required for response reduction over a wide frequency range. Large added masses are generally undesirable; otherwise they could be connected rigidly to the primary mass to reduce its response without introducing new resonances.

These conclusions, coupled with practical considerations such as the temperature dependence of the properties of viscoelastic materials, tend to rule out the desirability of vibration absorbers with viscoelastic springs.

2) Distributed Secondary System

It was thought that an absorber using a distributed mechanical system (such as a beam) instead of a rigid secondary mass m could be useful for controlling the vibrations of the primary mass at a number of frequencies. Detailed analyses of this idea showed that absorption could indeed be attained at many frequencies, but that such absorbers also result in resonances (and severe amplification of the responses) at frequencies very near the absorption frequencies. Such systems would therefore require very precise absorber design and accurate prediction of the exciting frequencies, and thus must be judged to be impractical in general.

B. Radiation Resistance Control in Beam Design*

Beams may be designed so that their flexural rigidities decrease with increasing frequency. They thus have higher coincidence frequencies than conventional beams with the same low-frequency (static) stiffness and should therefore result in less coupling to an acoustic field.

Two 44" x 24" test panels of 0.032" thick aluminum were constructed for this purpose. Three 24" long aluminum beams with C shaped cross-sections (0.065" thick 1.75" deep 1.0" flanges) were attached to one of the panels by means of an epoxy adhesive parallel to the 24" panel dimension and uniformly spaced over the 44" length. Three beams designed as indicated in Reference 19 of approximately the same static stiffness as the aluminum channels were similarly attached to the second panel. The coincidence frequency of the aluminum channels was calculated to be about 200 cps that of the latter type beams about 5 kc.

The results of measurements carried out on these two test panels appear in Fig. 9. The latter beams were found to produce lower values of radiation resistance R_{rad} and coupling factor μ than the more conventional channels. The near equality of the total resistances R_{tot} of the two panels indicates that the mechanical resistances R_{mech} of the two were nearly equal and considerably greater than the respective radiation resistances.

C. Viscoelastic Vibration Isolators

1. Leaf Springs

Viscoelastically damped beams may be designed according to available methods (refs. 2 20) to satisfy a considerable range of requirements and thus might provide superior broadband vibration isolation characteristics. An exploratory study of viscoelastic leaf springs was undertaken, therefore, as discussed in the following pages.

Consider a mass mounted symmetrically on two identical leaf springs. If a harmonic force of amplitude F acts on this mass. then a (rigid) support to which the springs are attached will also experience a harmonic force, but of amplitude F_o. Alternatively if the support is made to oscillate harmonically with an displacement amplitude Y_o. then the supported mass will oscillate with an amplitude Y. The transmissibility of a mounting system (here the leaf springs) is defined as

*The experiments described here use beams which are the subject of patent application by Bolt Beranek and Newman, Inc., and which bear the trade-mark "Soundshear". Properties and design of these structures are described in Reference 19.

FIG.9 TOTAL RESISTANCE R_{TOT}, RADIATION RESISTANCE R_{RAD} AND COUPLING FACTOR μ OF TEST PANELS WITH ATTACHED BEAMS OF SPECIAL DESIGN AND CONVENTIONAL CHANNELS

$$T = \left| \frac{F_o}{F} \right| = \left| \frac{Y}{Y_o} \right| \quad ; \tag{C.1}$$

the equivalence of the two ratios may be deduced from reciprocity (ref. 21).

The characteristics of beam-like structures depend on their boundary conditions. For the present analyses the leaf springs were assumed to be ideally clamped at the support and at the mounted mass. By solving the equation of flexural motions of elastic beams (refs. 4, 21) subject to the appropriate boundary conditions one finds that (ref. 22)

$$T = \frac{h(\alpha)}{f(\alpha) + \mu \cdot g(\alpha)} \tag{C.2}$$

where

$$\begin{aligned} h(\alpha) &= \sinh \alpha + \sin \alpha \\ f(\alpha) &= \cos \alpha \cdot \sinh \alpha + \sin \alpha \cdot \cosh \alpha \\ g(\alpha) &= \alpha(\cos \alpha \cosh \alpha - 1) \\ \alpha &= kL = 2\pi \cdot L/\lambda \\ \mu &= M/mL \quad . \end{aligned} \tag{C.3}$$

Here L denotes the length of one beam, m its mass per unit length, and M the supported mass per beam (or half the supported mass). Thus, μ denotes the ratio of supported mass to the mass of the supporting device. The symbol k denotes the wave number, λ the wavelength associated with free flexural waves in the beam:

$$k = 2\pi/\lambda = \sqrt[4]{m\omega^2/EI} \quad . \tag{C.4}$$

E denotes Young's modulus of the beam material, I the centroidal moment of inertia of the beam cross-section.

One may take damping into account by letting E take on complex values; that is, by replacing E by $E^* = E_1 + iE_2 = E_1 (1 + i\eta)$ where E_2 denotes the loss modulus, η the loss factor of the beam (refs. 2, 23). k and α also take on complex values k^* and α^*.

The general algebraic expressions tend to become intractable, but fortunately the mass ratios μ encountered in practical situations tend

to fall into two categories: 1) $\mu \ll 1$ (mass of leaf spring predominates) and 2) $\mu \gg 1$ (supported mass predominates). For these extreme situations one may arrive at some relatively simple approximations.

For $\mu \gg 1$ and small α (low frequencies) one finds that Eqs. (C.2) and (C.3) reduce to the classical transmissibility expression (refs. 22, 24) whose behavior is sketched in the insert of Fig. 10. For large α and large μ one obtains the approximation

$$\left|\alpha^*\right|\mu T \approx \left|\frac{\sin \alpha^* + \sinh \alpha^*}{\cos \alpha^* \cosh \alpha^* - 1}\right| \approx \left|\frac{1}{\cos \alpha^*}\right| . \qquad (C.5)$$

The second approximate equality applies for $|\alpha^*|$ not too small, - a condition which may be verified to apply where wave effects are important. If one introduces the parameters A and ϕ, defined so that

$$A = |\alpha^*| \quad , \quad \phi = \frac{1}{4} \arctan \eta \ , \quad \alpha^* = \alpha' - i\alpha'' = Ae^{-i\phi} \qquad (C.6)$$

then one finds that transmissibility peaks (standing wave resonances) occur where $\mathrm{Re}\{\cos \alpha^*\} = \cos \alpha' \cosh \alpha'' = 0$, or for

$$\alpha' = \pi(n + \tfrac{1}{2}) \quad , \quad n = 1, 2, \cdots . \qquad (C.7)$$

The magnitudes $\hat{T}$ of the transmissibility peaks are then given by

$$\mu\hat{T} \approx (A \sinh \alpha'')^{-1} \approx [\alpha_o \sinh (\alpha_o \sin \phi)]^{-1} . \qquad (C.8)$$

For most practical calculations one may determine the transmissibility peaks from Eqs. (C.7) and (C.8). In addition $A \approx \alpha'$ unless the damping is extremely high*, and practical calculations may be simplified further.

The validity of the approximations of Eqs. (C.7) and (C.8) may be verified from Fig. 10, in which the curves represent the results of calculations carried out by means of a digital computer (ref. 25) on the basis of the more exact expression Eq. (C.5) and the points marked by crosses represent values calculated from the approximations Eqs. (C.7) and (C.8)

For $\mu \ll 1$ and α not too small one similarly may write

$$T \approx \left|\frac{h(\alpha^*)}{f(\alpha^*)}\right| \approx \left|\frac{1}{\sin \alpha^* + \cos \alpha^*}\right| . \qquad (C.9)$$

This function exhibits peaks approximately where the real part of the denominator vanishes, or for

*For $\eta \leqslant 2.0$ one finds $1 \leqslant \alpha'/A \leqslant 1.04$.

$$\alpha' = \pi(n + \tfrac{3}{4}) \quad , \qquad n = 0,\ 1,\ 2,\ \cdots \tag{C.10}$$

The transmissibility peak values $\hat{T}$ may be found by substituting the foregoing values of α' into

$$\hat{T} \approx (2 \sin \alpha' \sinh \alpha'')^{-1} \approx [\sqrt{2} \sinh(\alpha_o \sin \phi)]^{-1}. \tag{C.11}$$

Figure 11 shows curves calculated from the more exact expression Eq. (C.9) and peak value points obtained from the foregoing approximations. Good agreement is again evident.

2. Axial Springs

It is instructive to compare the results obtained for leaf springs with similar results for axial (e.g., compression) springs. For the latter the general transmissibility expression may be written as (refs. 22, 26)

$$\begin{aligned} T &= |\cos \beta - \mu' \beta \sin \beta|^{-1} \\ \beta &= \omega \sqrt{mH/K} \\ \mu' &= M/mH \end{aligned} \tag{C.12}$$

where m denotes the mass per unit length, H the equilibrium length of the spring, K the classical spring constant, and μ' the ratio of supported mass to total spring mass.

One may again introduce damping effects by replacing K by an appropriate complex quantity $K^* = K_1 + iK_2 = K_1(1+i\eta)$; then β also takes on complex values:

$$\beta^* = \beta' - i\beta'' = Be^{-i\gamma} \quad , \quad B = |\beta^*| \ , \ \gamma = \tfrac{1}{2} \arctan \eta \tag{C.13}$$

One again finds that for large mass ratio μ' and low frequencies (small β^*) Eqs. (C.12) reduce to the classical transmissibility result (ref. 22). For β^* not too small and large μ Eq. (C.12) may be replaced by the approximate relation

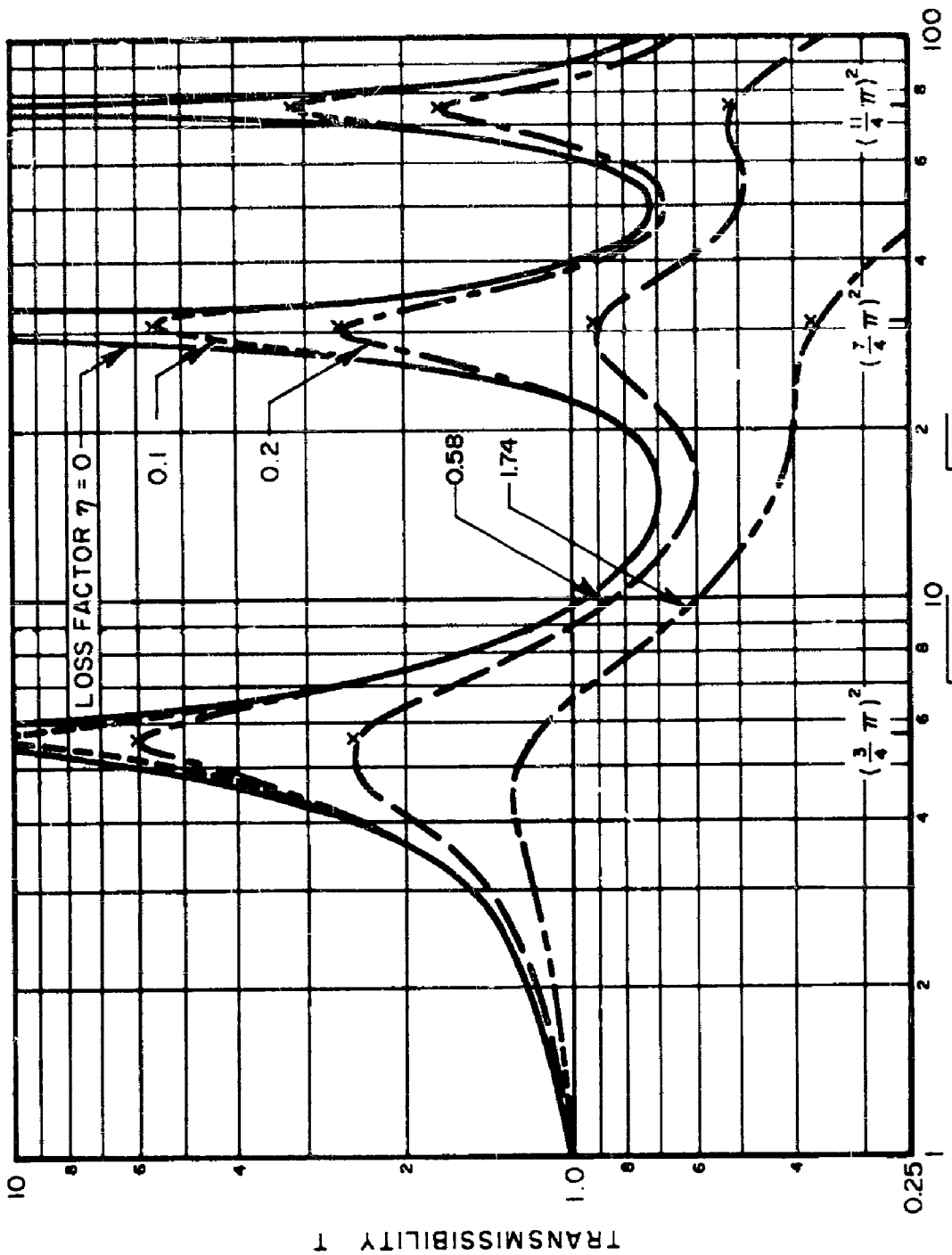

FIG. 11 TRANSMISSIBILITY OF VISCOELASTIC LEAF SPRING FOR SMALL MOUNTED MASS ($\mu << 1.0$)

$$|\beta^*|\mu' T \approx |\sin \beta^*|^{-1} \tag{C.14}$$

which implies transmissibility peaks given by

$$\mu' \hat{T} \approx (B \sinh \beta'')^{-1} \approx [B \sinh (B \sin \gamma)]^{-1} \tag{C.15}$$

where

$$\beta' \approx n\pi , \qquad n = 1, 2, \cdots \tag{C.16}$$

Similarly, for small mass ratio μ',

$$T \approx |\cos \beta^*|^{-1} , \tag{C.17}$$
$$\hat{T} \approx |\sinh \beta''|^{-1} = [\sinh (B \sin \gamma)]^{-1}$$

and peaks occur where

$$\beta' \approx \pi(n + \tfrac{1}{2}) , \qquad n = 1, 2, \cdots \tag{C.18}$$

The validity of these approximations may be inferred from Figs. 12 and 13, in which the curves represent the results of the more exact calculations and the points represent results obtained by means of the foregoing approximate expressions.

3. Comparison

It may be shown that if leaf springs and compression springs are to have the same ratio of supported mass to support mass and the same classical fundamental natural frequency, then the previously defined parameters A and B must be related as

$$A^2 = B\sqrt{12} . \tag{C.19}$$

Figures 11 and 12 are scaled to conform to Figs. 9 and 10 on this basis, so that one may compare leaf springs and common springs equitably by comparing these sets of figures.

On the basis of these figures, or by means of mathematical analysis of the pertinent relations, one may conclude that compared to compression springs of equivalent mass and damping, leaf springs

1) result in fewer transmissibility peaks for a given frequency range; but

2) tend to result in a generally higher level of transmissibility between peaks and in a higher envelope of transmissibility peaks.

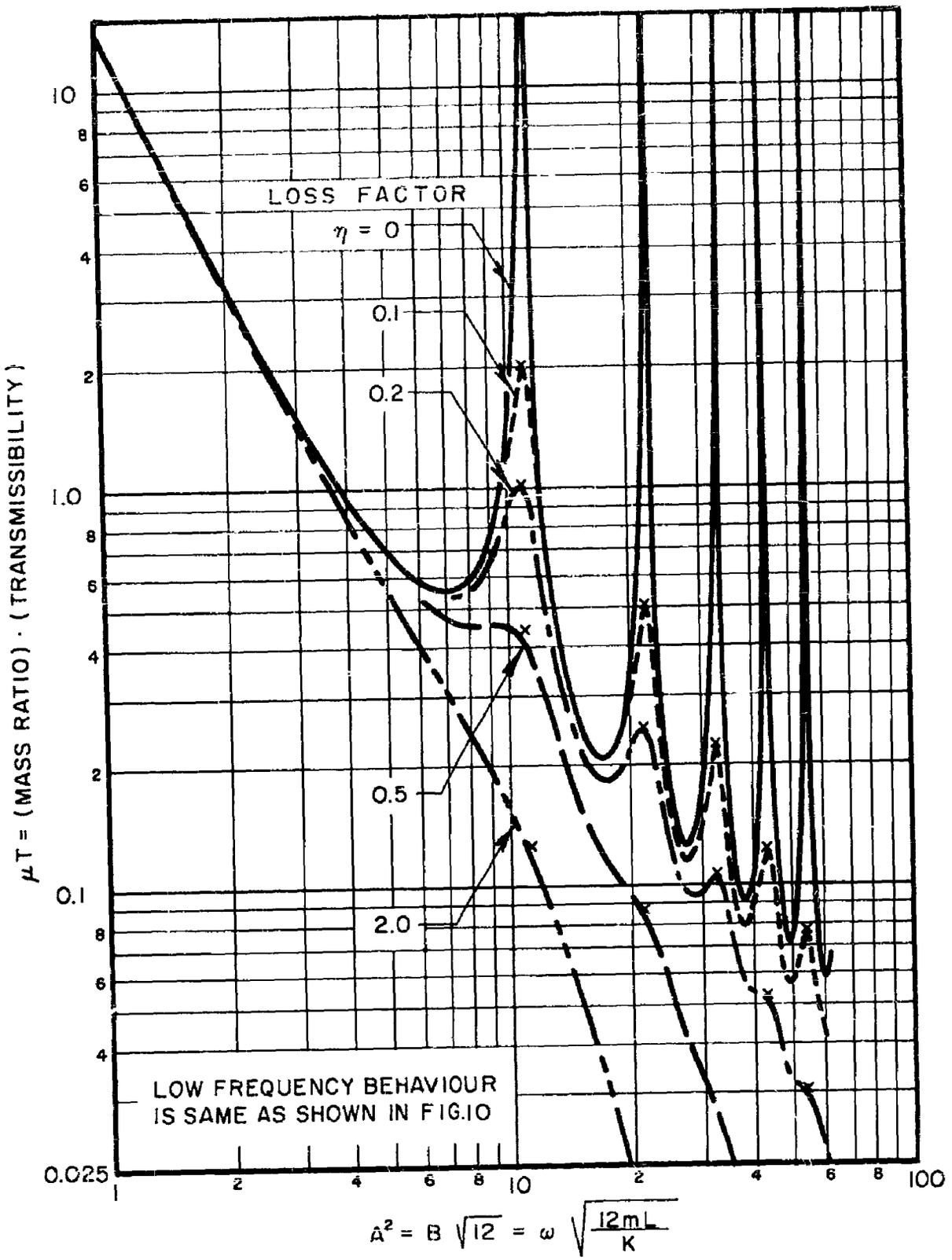

FIG.12 TRANSMISSIBILITY OF VISCOELASTIC COMPRESSION SPRING FOR LARGE RATIO μ' OF MOUNTED MASS TO SPRING MASS

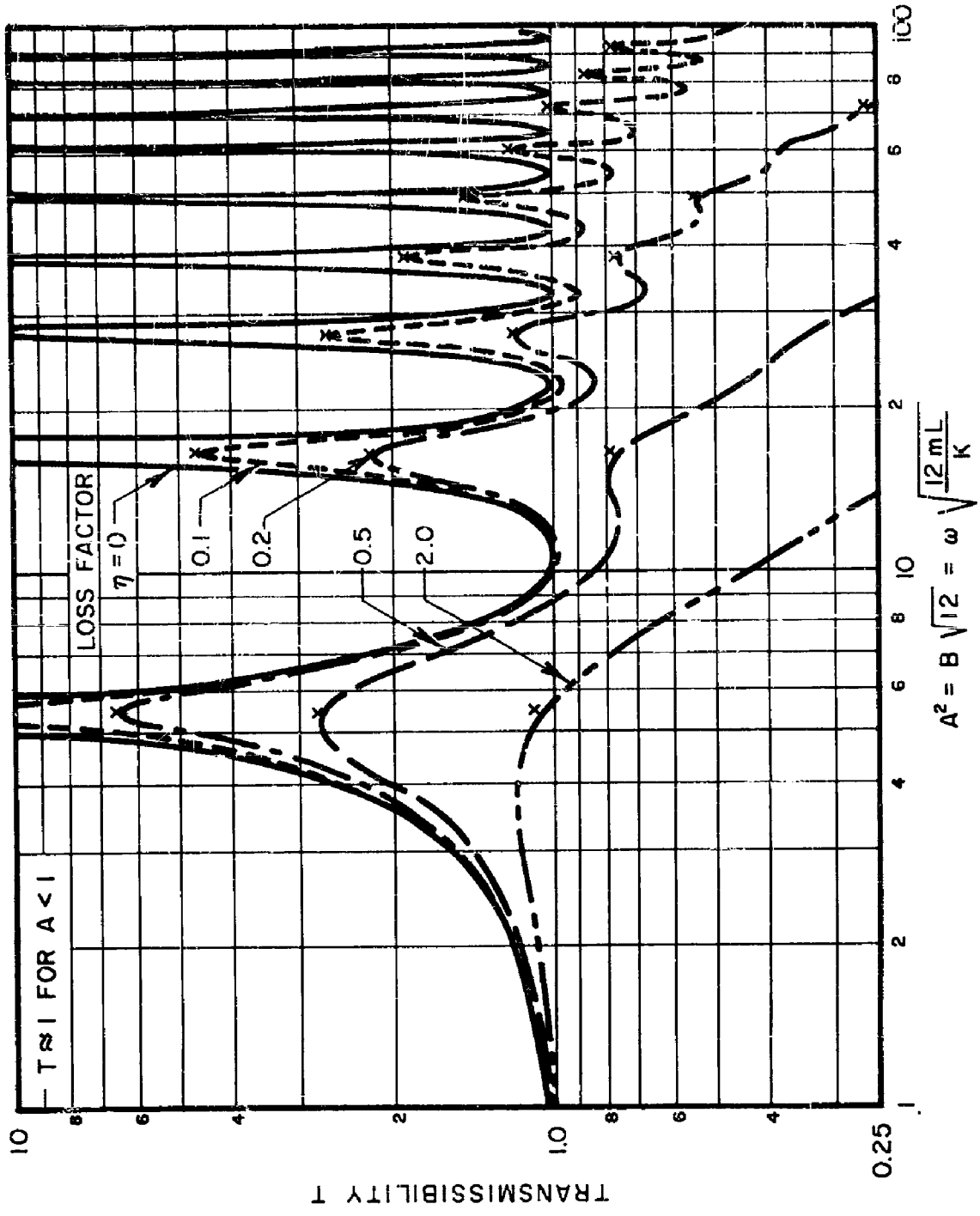

FIG.13 TRANSMISSIBILITY OF VISCOELASTIC COMPRESSION SPRING FOR SMALL MOUNTED MASS ($\mu'<<1.0$)

One should note, however, that the present state of the art permits large amounts of damping to be designed into leaf springs more readily than into compression springs, and that viscoelastically damped leaf springs may thus constitute superior broadband vibration isolation devices.

D. Damping of Beam-Plate Systems

Since aircraft and other structures consist primarily of beams and plates, the reduction of the vibrations of such beam-plate systems has received considerable attention. The addition of damping structures and materials usually results in weight increases, so that it is desirable to apply such damping treatments as conservatively as possible and only where they will do the most good. The subsequently outlined study was undertaken, therefore, as an attempt to define under what conditions damping of only the beams is preferable to damping of only the plates, and vice versa.

The system studied is sketched in Fig. 14. Although this sketch shows a rectangular plate and the subsequent discussion deals in Cartesian coordinates, these restrictions are not necessary; the conclusions of the study should be more generally applicable. However, it must be assumed that the boundary conditions of the beam are the same as those of the plate at those plate edges which coincide with the beam ends.

1. Separable Eigenfunctions

Sinusoidal free motion of a plate at frequency ω may be described by $w(x,y)e^{i\omega t}$, where $w(x,y)$ denotes the deflection shape and obeys the classical equation (refs. 21, 27).

$$D\nabla^4 w - \mu\omega^2 w = 0 \quad , \tag{D.1}$$

where D denotes the flexural rigidity of the plate, μ its mass per unit area. For a given set of plate boundary conditions one may find a doubly infinite set of solutions $w = \psi_{mn}(x,y)$ that, in conjunction with $\omega = \omega_{mn}$, satisfy Eq. (D.1) and the prescribed boundary conditions.

Forced motion of the plate may be described by the addition of a term $p(x,y)$ on the right-hand side of Eq. (D.1). The plate response $w(x,y)$ and forcing pressure distributions may be expressed in terms of eigenfunction series*

---

*All double summations extend over $m,n, = 1,2, \cdots, \infty$.

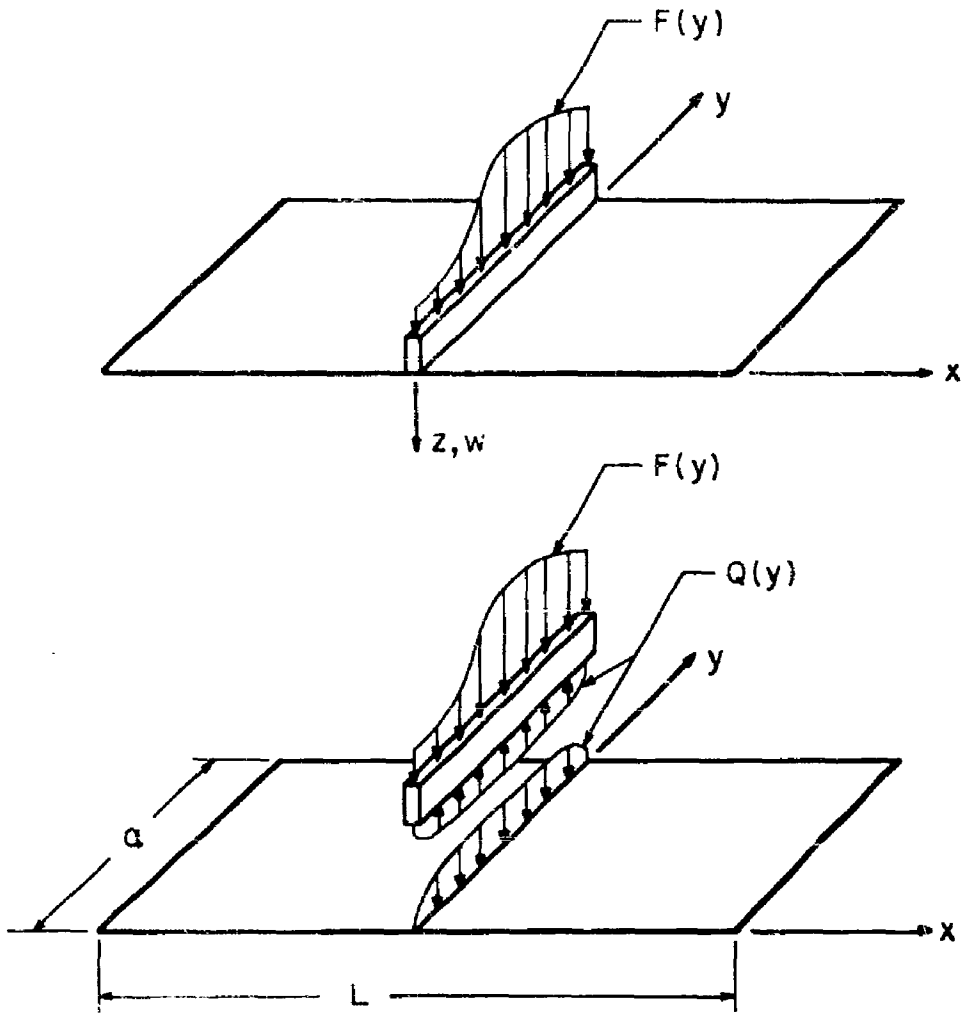

FIG. 14 BEAM-PLATE INTERACTION

$$w(x,y) = \sum\sum W_{mn}\, \psi_{mn}(x,y) \quad , \quad p(x,y) = \sum\sum P_{mn}\, \psi_{mn}(x,y) \quad , \qquad (D.2)$$

whose coefficients are related as (ref. 28)

$$W_{mn}\, \mu \left[\omega_{mn}^2 (1 + i\delta) - \omega^2 \right] = P_{mn} \qquad (D.3)$$

if damping of the plate is also taken into account by replacing the real parameter D of Eq. (D.1) by the complex parameter $D^* = D(1 + i\delta)$; δ denotes the loss factor of the plate.

A useful special case occurs if the eigenfunctions ψ_{mn} can be expressed as products of separate functions of the two plate coordinates:

$$\psi_{mn}(x,y) = f_m(x)\, g_n(y) \quad . \qquad (D.4)$$

For the usual ideal boundary conditions (clamped, free, or supported) the ψ_{mn} are orthogonal; hence the factor functions are also orthogonal, and one may write

$$\int_L f_m(x)\, f_{m'}(x)\, dx = \begin{cases} L\Phi_m & \text{for } m = m' \\ 0 & \text{for } m \neq m' \end{cases}$$

$$\int_a g_n(y)\, g_{n'}(y)\, dy = \begin{cases} a\Gamma_n & \text{for } n = n' \\ 0 & \text{for } n \neq n' \end{cases} \qquad (D.5)$$

where Φ_m and Γ_n are constants, and the indicated integrations are carried out over the plate edge lengths.

2. Beam-Plate Interaction; Excitation at Beam

The force distribution Q(y) acting between the beam and the plate may be interpreted as a pressure distribution $p(x,y) = Q(y)\, \Delta(x)$, where Δ denotes the Dirac delta function. The plate deflection due to Q(y) may then be obtained by application of the foregoing result. In particular, the plate deflection at the beam (at $x = 0$), which is also the beam deflection and is denoted here by z(y), is found to be given by

$$z(y) = \sum_n Z_n g_n(y) \quad , \qquad Z_n = \frac{Q_n}{\mu L} (K_n - i\Lambda_n) \qquad (D.6)$$

where (analogously to ref. 29),

$$K_n = \sum_m \frac{f_m^2(o)}{\Phi_m} \frac{h/\omega_{mn}^2}{h^2+\delta^2} \quad , \quad \Lambda_n = \sum_m \frac{f_m^2(o)}{\Phi_m} \frac{\delta/\omega_{mn}^2}{n^2+\delta^2} \quad , \qquad (D.7)$$

$$h \equiv 1 - (\omega/\omega_{mn})^2$$

and Q_n is obtained from the expansion $Q(y) = \sum_n Q_n g_n(y)$.

The beam deflection z, however, must satisfy the beam's equation of motion (refs. 21, 27)

$$B^* \frac{d^4 z}{dy^4} - M\omega^2 z = F(y) - Q(y) \qquad (D.8)$$

where $B^* = B(1 + i\beta)$ denotes the beam's (complex) flexural rigidity, M its mass per unit length, and where F(y) denotes an externally applied force distribution as shown in Fig. 14. If this external force is also expanded as $F(y) = \sum_n F_n g_n(y)$, one may obtain the following relation between modal force F_n and modal beam deflection Z_n:

$$\frac{F_n}{Z_n} = M\left[\omega_n^2 (1+i\beta) - \omega^2\right] + \mu L \frac{K_n + i\Lambda_n}{K_n^2 + \Lambda_n^2} \quad . \qquad (D.9)$$

Here ω_n denotes the beam's n^{th} natural frequency, which may be shown to obey

$$\omega_n^2 = C_n^4 \frac{B}{M} \quad , \quad C_n^4 = \frac{1}{g_n} \frac{d^4 g_n}{dy^4} \quad , \qquad (D.10)$$

where C_n is a constant [as a consequence of Eq. (D.4)]

In absence of damping ($\beta = \delta = 0$), infinite amplitudes Z_n result for finite driving force F_n (i.e., resonance occurs) whenever $\mathrm{Re}\left\{F_n/Z_n\right\} = 0$ in Eq. (D.9). Damping of practically feasible magnitudes

generally changes the resonance frequencies only slightly, so that for all practical purposes one may still assume that the real part of Eq. (D.9) vanishes at resonance. Then, in the presence of damping, at resonance

$$\left|\frac{F_n}{Z_n}\right|_{Res} \approx M\omega_n^2\beta + \frac{\mu L \Lambda_n}{K_n^2+\Lambda_n^2} \qquad (D.11)$$

Of the terms on the right-hand side of Eq. (D.11) the first represents the damping effect of the beam, the second that of the plate. From Eqs. (D.7) one finds that significant contributions to Λ_n occur only for $\omega \approx \omega_{mn}$. The optimum damping effect of the plate on oscillations driven at the beam hence may be realized if one designs the beam-plate system so that its resonances coincide with those of the plate.* For such an optimized system $\omega_n = \omega_{mn}$ and

$$\left|\frac{F_n}{Z_n}\right|_{Res} \approx \omega_n^2 \left(M\beta + \mu L \frac{\Phi_m}{f_m^2(0)}\delta\right) \qquad (D.12)$$

For many (rectangular) systems one may, at least in theory, design the plate so that it has a resonance wherever the beam has a resonance. For a simply supported system with a centrally located beam one finds that $\omega_n = \omega_{mn}$ if

$$1 + \left(\frac{m}{n}\frac{a}{L}\right)^2 = \sqrt{\frac{B\mu}{DM}} \quad . \qquad (D.13)$$

In order for a plate resonance to correspond to each beam resonance the foregoing equation must be satisfied for each value of n, n = 1,2,3,$\cdots$. One thus needs merely to select some design value α for the ratio m/n, then choose the beam and plate dimensions according to Eq. (D.13). (If Eq. (D.13) is to hold for all n, α must be an integer.)

---

*Heckl (ref. 8) obtained this conclusion by considering the plate as an array of rods and demonstrated its validity experimentally.

3. Excitation on Plate

In the presence of an externally applied pressure $r(x,y)e^{i\omega t}$ acting on the plate, one may write the modal loading P_{mn} of Eq. (D.2) as

$$P_{mn} = R_{mn} + \frac{f_m(0)Q_n}{L\Phi_m} \tag{D.14}$$

where the first term denotes coefficients of $r(x,y)$ and the second denotes the contribution of the beam-plate interaction force $Q(y) = \sum_n Q_n g_n(y)$. From Eq. (D.8) with $F(y) = 0$ one may establish a relation between Q_n and the modal beam deflection Z_n; the latter also obeys

$$Z_n = \sum_m W_{mn} f_m(0) \tag{D.15}$$

in view of the definition of modal deflection W_{mn} of Eq. (D.2). Combination of these results with Eq. (D.3) then permits one to arrive at the following relation between modal pressure R_{mn} and modal deflection W_{mn}:

$$\frac{R_{mn}}{\mu W_{mn}} = (1+i\delta)\omega_{mn}^2 - \omega^2 + J_m\,[(1+i\beta)\omega_n^2-\omega^2] \sum_s \frac{W_{sn}}{W_{mn}} \frac{f_s(0)}{f_m(0)} \tag{D.16}$$

$$J_m \equiv \frac{M}{L\mu} \frac{f_m^2(0)}{\Phi_m}$$

Equation (D.16) represents an infinite set of simultaneous equations. Solution is difficult since the equations are coupled, as evident by the appearance of all W terms on the right-hand side. Fortunately, however, one need not attempt a solution to discuss resonant behavior of the system.

At resonance of the m,n mode the modal amplitude W_{mn} may be expected to exceed all others considerably. System resonances may be expected to occur for $\mathrm{Re}\{R_{mn}/W_{mn}\} = 0$, or at frequencies Ω_{mn} given by

$$\Omega_{mn} \approx \frac{\omega_{mn}^2 + J_m\,\omega_n^2}{1 + J_m} \tag{D.17}$$

The resonant modal displacement then obeys

$$\left|\frac{R_{mn}}{\mu W_{mn}}\right|_{Res} \approx \delta\omega_{mn}^2 + \beta J_m \omega_n^2 \quad , \qquad (D.18)$$

The first term represents the plate contribution, the second that of the beam; J_m may be seen to describe essentially the coupling of the n-mode of the beam to the m,n-mode of the plate.

4. Conclusions

Beam resonant responses may be reduced by damping the attached plates. Optimum effective beam damping is obtained when the plate resonances are made to coincide with the beam resonances. For some configurations this matching may be accomplished for all beam resonances by suitable adjustment of the beam and plate geometries.

On the other hand, beam damping has generally less effect on the resonant responses of plates. Only a stiff, massive, and highly damped beam can have much influence on the resonant responses of a plate. But even such beams have little effect on those modes for which the beam is located near a nodal line of the plate, or for which plate flexure perpendicular to the beam predominates.

E. Damping of Aircraft Structural Joints

As discussed in the first section of this report, the damping at joints may be important in controlling the vibrations of a structure. Increases in the damping at joints might be obtainable with relatively minor structural modifications, which might thus provide a simple and economical means for reducing vibratory response of the structure. This section summarizes the results of an exploratory study aimed at gaining some understanding of the mechanisms responsible for the damping in riveted and similar joints; such understanding is clearly necessary for rational optimization of this damping.

Some studies of similar problems have pointed toward the importance of Coulomb or dry friction damping in some structural joints. For example Klumpp and Goodman (ref. 30) developed analyses for press-fit joints, and Pian (ref. 31) investigated built-up beams. These studies showed good agreement between experimental measurements and theoretical predictions based on Coulomb damping; strong dependences of damping on amplitude (i.e., nonlinearities) were found. Somewhat different results were reported by Mead (ref. 32). In experiments performed on more nearly practical riveted joints he observed no amplitude dependence of damping, except at relatively high amplitudes (which are of lesser interest here, since one desires to avoid severe vibrations in the first place).

As Mead has pointed out, the damping of riveted joints might be affected by many factors, including:

1. Amplitude and mode shape of the vibration.

2. Normal pressure between joined structures and its distribution about rivets.

3. Shear stiffness of rivet in relation to local stiffness of joined structures. End fixity of rivets associated with rivet head geometry, radial pressure between rivet and hole; i.e., assembly methods, might make significant differences.

4. Surface conditions at the interface, including roughness, presence of lubricants, dust, local oxidation, wear (fretting).

In order to assess the importance and trends associated with some of these parameters, a number of damping measurements were undertaken using essentially the experimental setup described by Kerwin (refs. 33, 34). The measurements consisted of driving a test bar sinusoidally, removing the excitation, and observing the decay of the vibration. From an oscilloscope display of the logarithm of amplitude versus time the linearity of the decay could be assessed directly, and the loss factor could be obtained from the slope of the decay curve by means of a simple calculation (ref. 34).

1. Experimental Results

A preliminary experiment was performed on two 1/8" thick 24ST aluminum plates, 2" wide and 15.5" long, joined by 8 bolts (arranged 4" apart in two parallel rows, with 1" between rows). The decay curves were observed to be straight, i.e., damping was found to be linear, over the entire range of amplitudes (0.02 to 50 g) of the experiment. Similar linearity was also observed in virtually all of the subsequently reported experiments, but in most of these no attempt was made to obtain a wide range of amplitudes.

A series of damping measurements were carried out on test pieces cut from the interior of the forward structure of an F-105 aircraft. These test samples, whose cross-sections are sketched in Fig. 15, consisted of 27 inch long beams with sections of skin attached by rivets or spot welds. Test results for these samples appear in Fig. 15, together with results pertaining to the riveted sample piece after the rivets had been drilled out and replaced by bolts and nuts. From these results it appears plausible that the different joining methods considered result in essentially the same damping if the geometries of the joints are roughly similar. Since Fig. 15 pertains to methods that produce tight joints, i.e., that produce good connections in the vicinity of the connectors, the foregoing statement might be extended to include any tight joint. It thus appears that the damping of such tight joints is not due to the connectors themselves, but perhaps due to relative motion at the interface at some distance from the connectors.

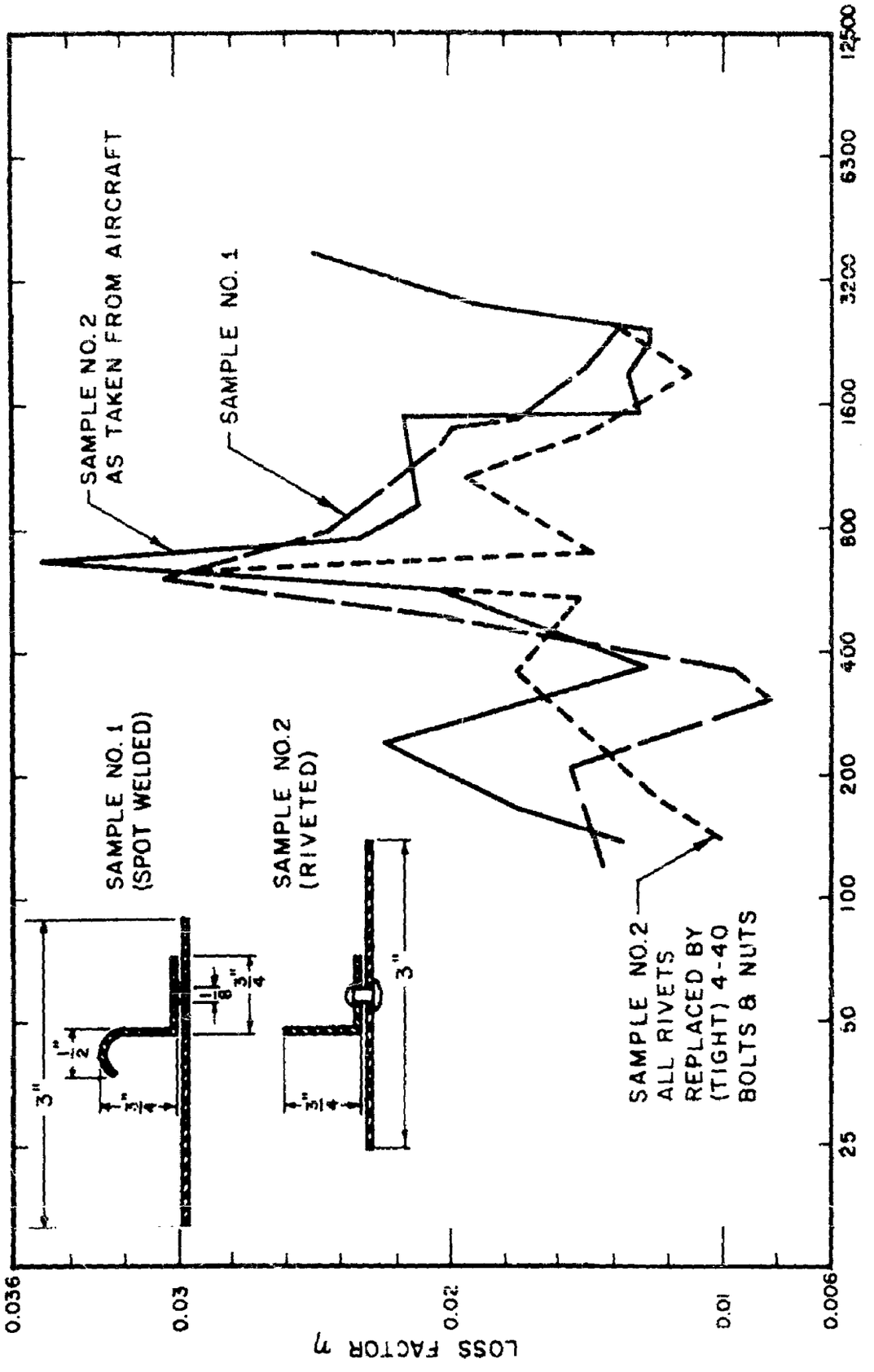

FIG.15 SIMILARITY OF DAMPING OF TIGHT JOINTS

In view of Fig. 15, one may also expect to be able to obtain results that have some meaning in relation to riveted joints from experiments conducted on bolted joints, which are much easier to adjust to desired conditions. Figure 16 marshals additional data in support of the similarity of the damping characteristics of riveted and bolted joints. (No torque wrench was available for the small, 4-40, screws that were used. The "tight" condition corresponds to the tightest that could be obtained by hand with a screwdriver; the "loose" was obtained by backing the screws off one quarter turn from the tight condition.)

Effects of rivet spacing may be seen in Fig. 17, which summarizes the damping results obtained for the aforementioned riveted aircraft joint sample before and after drilling out some of the rivets. Again, since damping is certainly not proportional to the number of rivets, it cannot be due to the rivets per se or to small areas surrounding the rivets. It may be more reasonable to associate damping with relative motion at interface areas located outside of "clamped" areas near connectors. From the near correspondence of the curve for 38 to that for 18 rivets one might estimate that in the original sample the clamped areas associated with adjacent rivets probably overlapped.

That damping can not be associated merely with the structure in the immediate neighborhood of the connectors is also evident from Fig. 18. The curves of this figure pertain to the spot-welded sample structure, with different widths of the skin portions (corresponding to the 3" dimension of Fig. 15). Since the identical connections are involved in all the cases shown here; they hence cannot be responsible for the changes observed, and one is once again led to ascribe the damping to those portions of the structure which are not near the spot welds.

Figures 19 and 20 illustrate the effects of interface lubrication. The addition of lubricant was found to result in increased damping, with less viscous lubricants producing higher damping.* Comparison of these two figures also indicates that reduction of interface pressure (loosening of the screws) results in increased damping for all of the interface conditions tested. Pressure reduction and improved lubrication thus produce similar results, probably

---

*It should be noted that some lubricant was found in the joint as cut from the aircraft; the corresponding damping curve is labeled "original condition". Chemical degreasing resulted in reduced damping, and subsequent chemical removal of the zinc chromate coating (curve labeled cleaned to metal) lowered the damping even more.

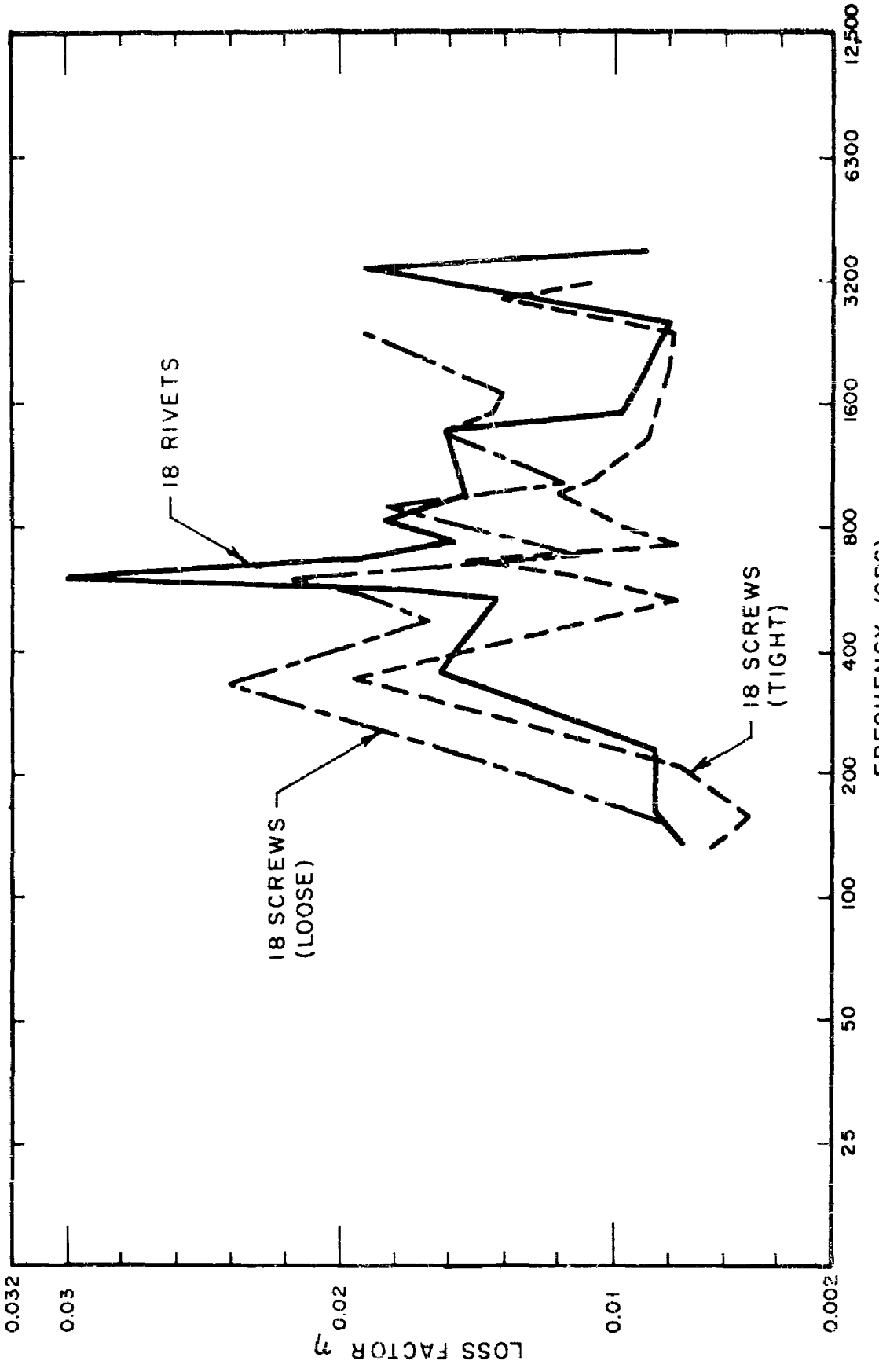

FIG. 16 COMPARISON OF RIVETS AND VARIOUSLY TIGHTENED SCREWS (SAMPLE NO. 2)

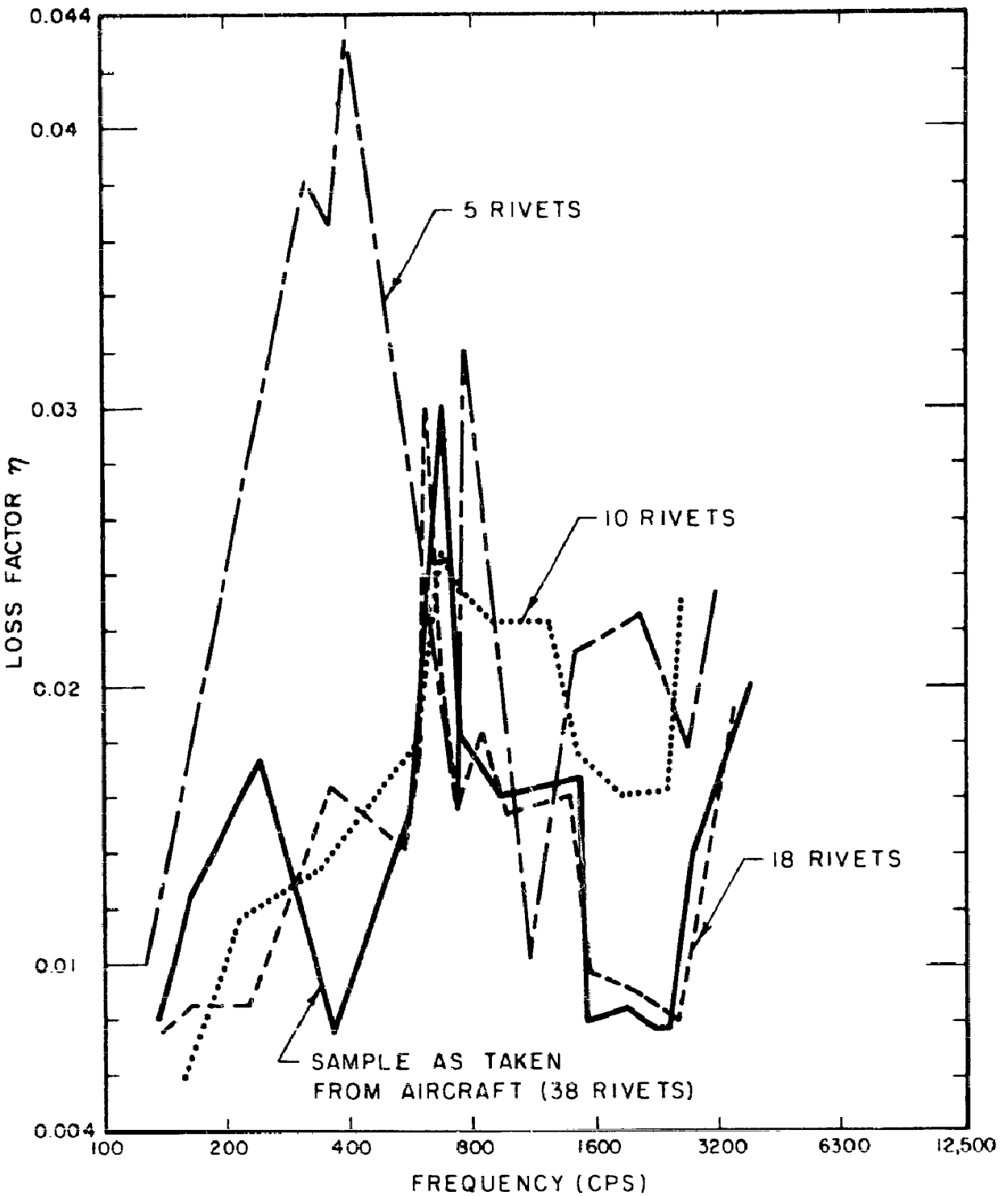

FIG. 17 EFFECT OF RIVET SPACING (SAMPLE NO. 2)

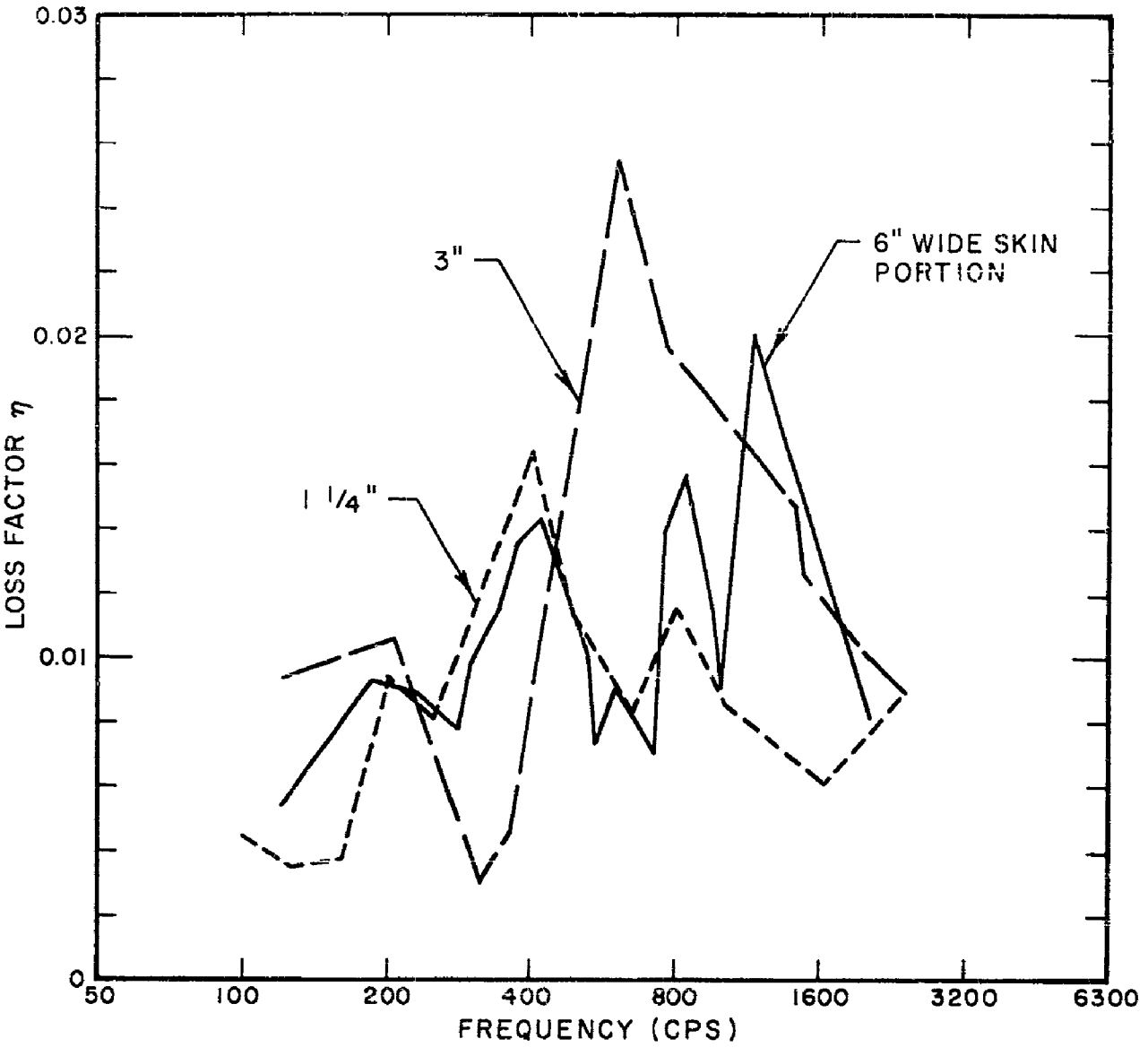

FIG. 18 EFFECTS OF WIDTH OF ATTACHED SKIN PORTION (SAMPLE NO. 1)

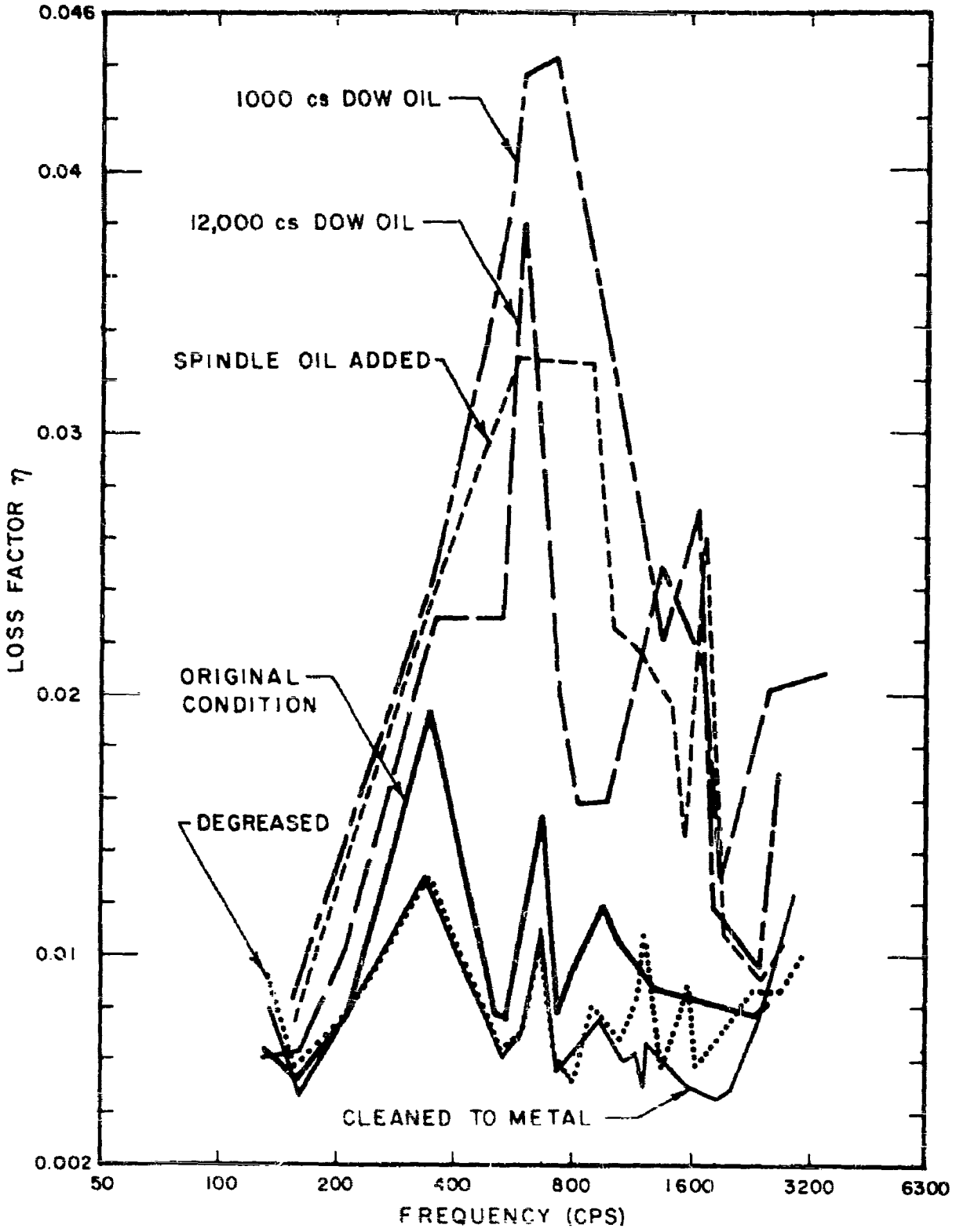

FIG. 19 EFFECTS OF INTERFACE LUBRICATION (SAMPLE NO.2 WITH 18 SCREWS, TIGHT)

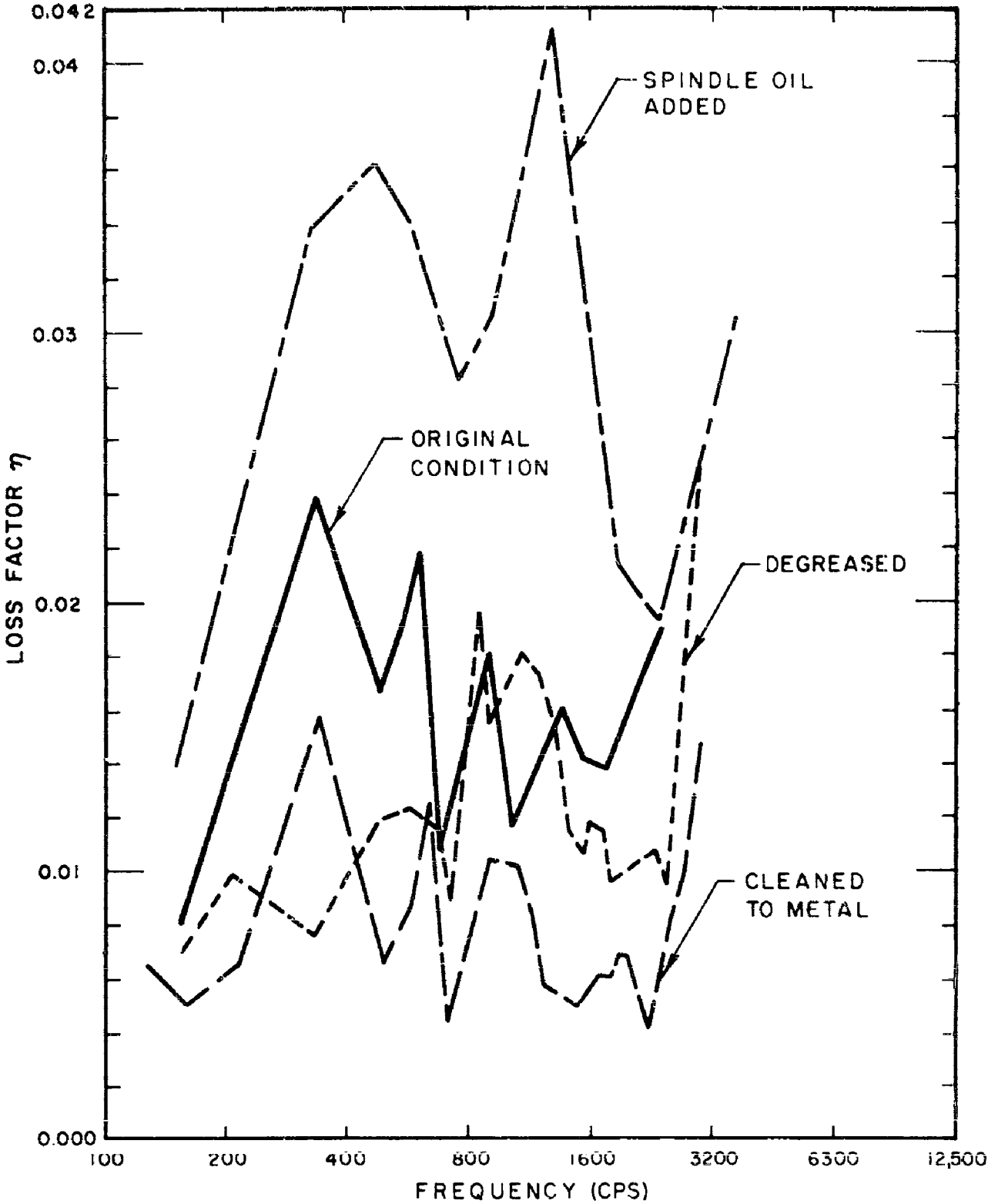

FIG.20 EFFECTS OF INTERFACE LUBRICATION (SAMPLE NO.2 WITH 18 SCREWS, LOOSE)

since both serve to reduce interface friction. Reduced friction results in increased relative motion, which evidently more than compensates for the effect of the reduced friction as far as energy dissipation is concerned. (Note that the cyclic energy dissipated in a classical linear dashpot is proportional to the square of the amplitude, but only to the first power of the viscous damping coefficient.)

Figure 21 shows the results that some simple modifications had on the damping of the riveted F-105 sample structure. With the toe of the original equilateral L-shaped cross-section bent down a general increase in damping was observed, which may at least in part be attributed to the extremely good contact fostered by such a cross-section at the heel and toe of the L. However, a further general increase in damping was obtained (except below 630 cps) when the toe of the L was cut off altogether. This increase might be due to improved contact in the area that previously was between the heel and toe; such improvement would be most noticeable at the higher frequencies, where the motion is less restricted by the "rivets". The peak observed at about 500 cps with the bent-down toe is probably due to a mode shape for which a considerable amount of relative motion occurs at the toe.

Figures 22 and 23 summarize results of experiments aimed at evaluating the effects of beam-and-skin contact area and of beam stiffness separately. The measurements indicated in these figures were performed on specially designed aluminum channel beams; those of Fig. 22 have nearly the same flexural rigidity but differ considerably in contact area, whereas those of Fig. 23 have equal contact areas but different stiffnesses.

Increased contact area was found to result in increased damping and changes in beam stiffness were found to affect damping relatively little in general. The picture is by no means clear, however. It is difficult to say, for example, if the higher damping noted with increased contact area is due to this area increase *per se* or to changes in mode shape. The high peaks shown in Fig. 23 between 500 and 800 cps also present somewhat of an anomaly. Calculations show that this frequency range corresponds to that where one half wavelength of flexural motion of the skin is equal to the width of the skin attached to the test beams, so that these peaks might be due to bending of the composite *about* the rivet line (in contrast to the rest of the curve which probably is primarily associated with bending *of* the rivet line).

A final series of tests were performed to determine the effects of adhesives. The results of these tests, as shown in Fig. 24, indicate that a dissipative adhesive like MMM 466 can result in a considerable damping increase over a wide frequency range, whereas a relatively rigid loss-less adhesive (epoxy) not only adds little damping but even reduces the damping of riveted joints under some circumstances.

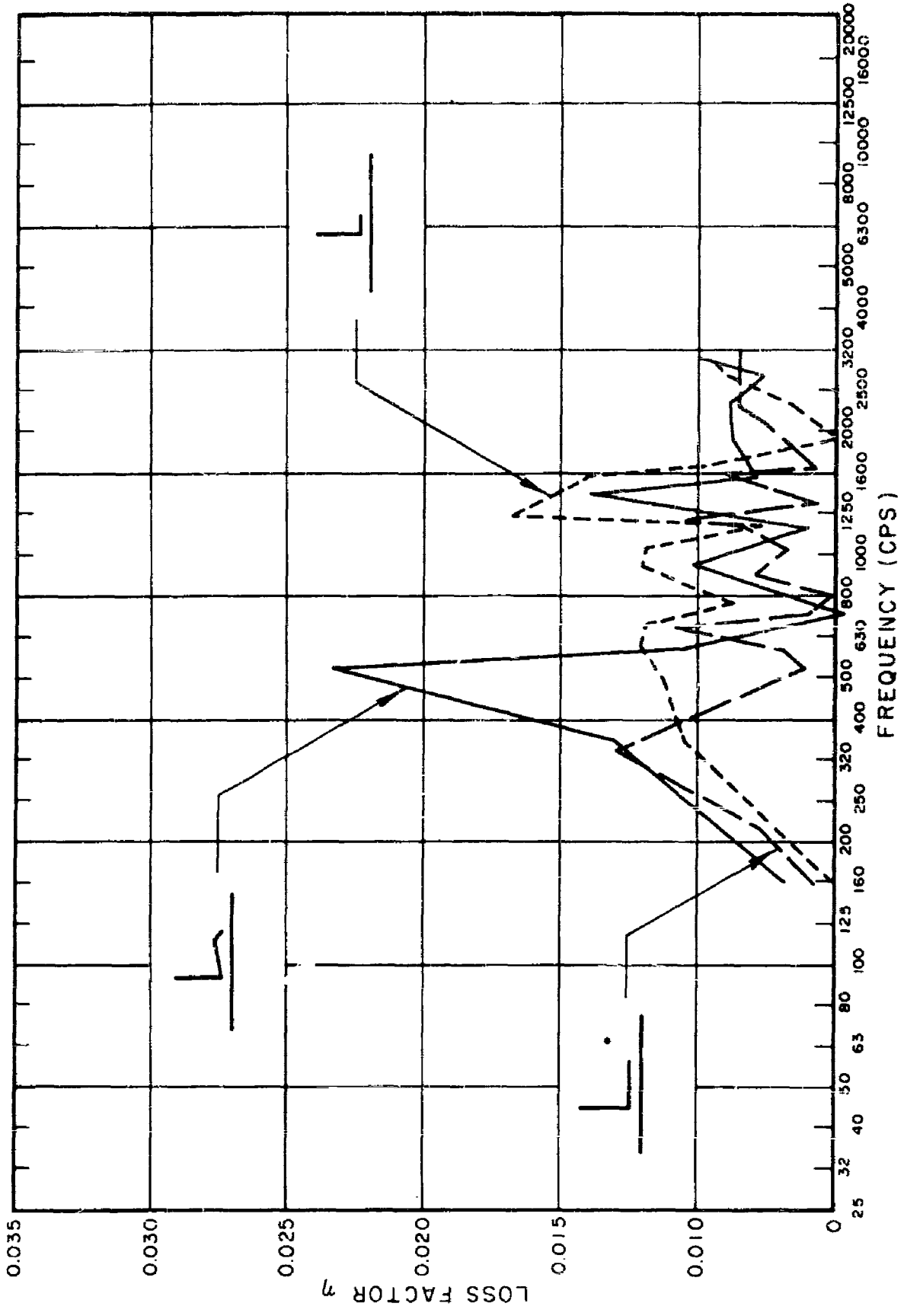

FIG. 21 EFFECTS OF CONTACT AREA MODIFICATIONS OF SAMPLE NO. 2.
(CLEAN INTERFACE, 18 SCREWS, TIGHT)

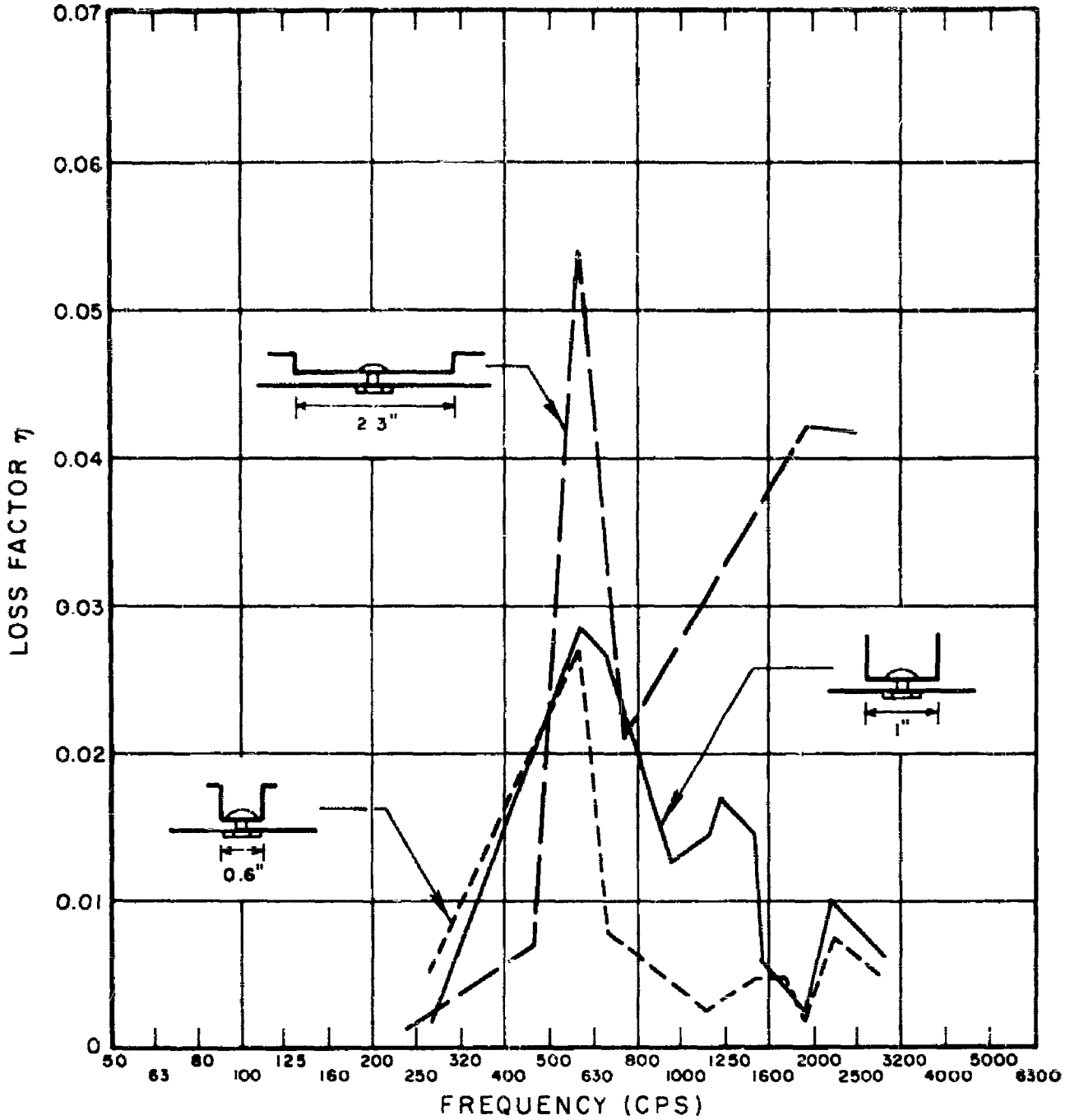

FIG. 22 EFFECT OF CONTACT AREA ON DAMPING OF BOLTED JOINT.

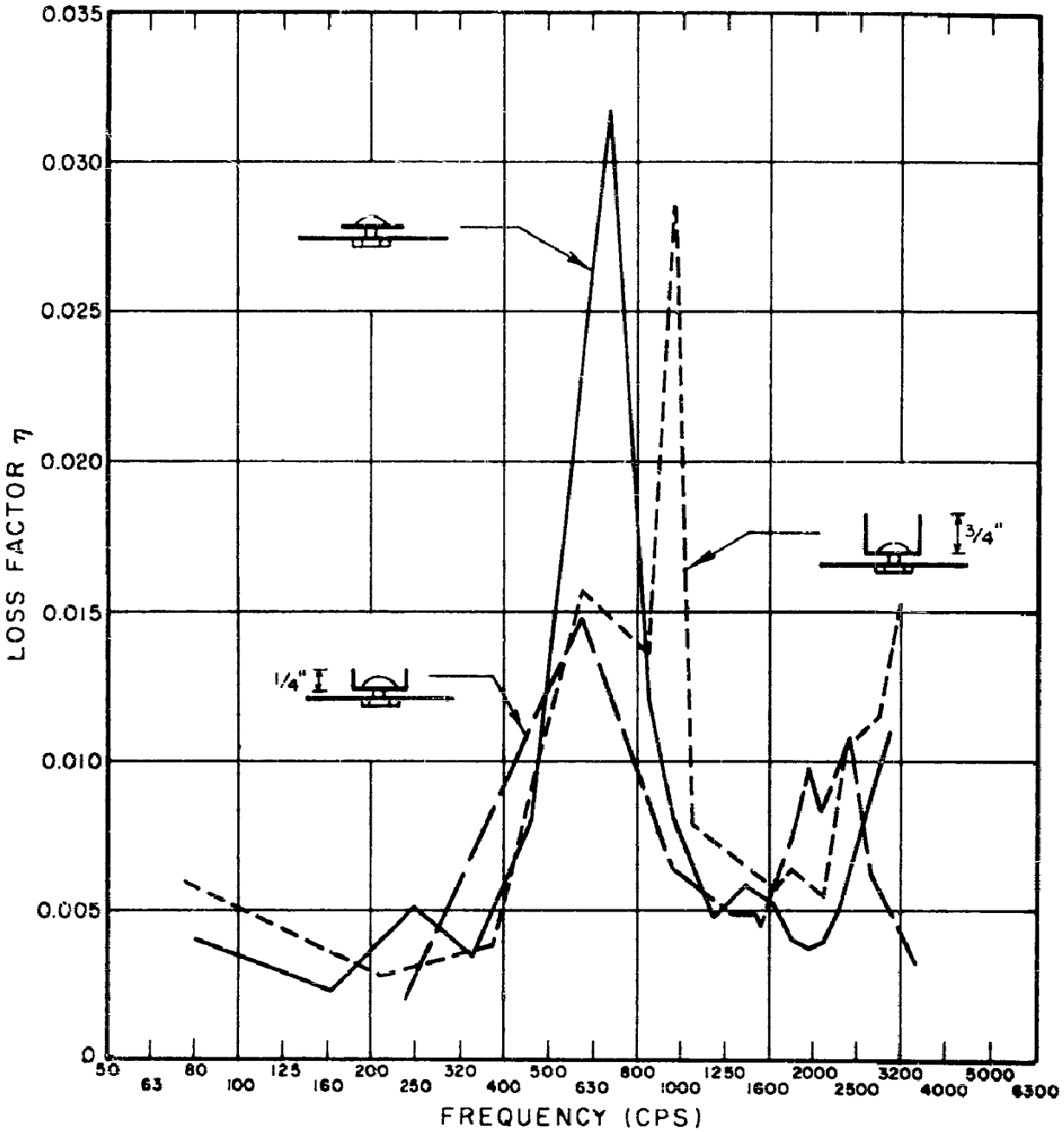

FIG.23 EFFECT OF BEAM STIFFNESS ON DAMPING OF BOLTED JOINT.

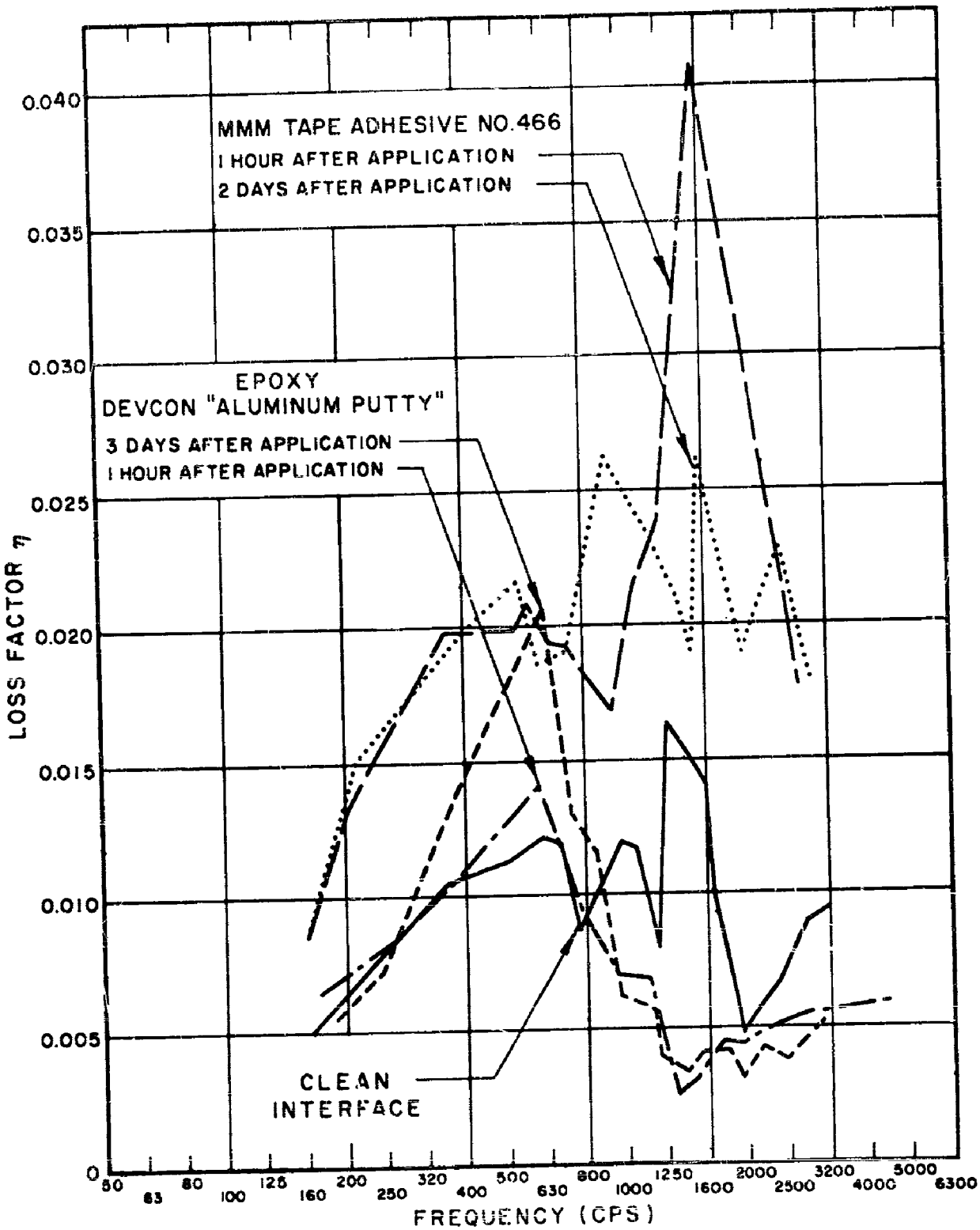

FIG.24 EFFECTS OF ADHESIVES AT INTERFACE (SAMPLE NO.2 WITH REDUCED CONTACT AREA; 18 SCREWS TIGHT)

2. Conclusions

The studies outlined here, although by no means conclusive or as comprehensive as one would like, permit one to arrive at least at some tentative conclusions.

These are:

1. The damping of aircraft joints is essentially linear, except perhaps at high amplitudes.

2. The damping of tight joints seems not to be primarily associated with the connectors or the structure in the immediate vicinity of the connectors.

   a. Different connectors (spot weld, rivets, bolts) produce similar damping characteristics.

   b. Studies on bolted joints are capable of yielding results that have some meaning in relation to riveted joints.

3. Looser joints produce higher loss factors; reduced interface pressure (looser or fewer rivets) or better lubrication results in higher damping.

4. Increased beam-to-skin contact area produces increased damping.

5. Beam stiffness *per se* has relatively little effect on damping.

6. Rubbery dissipative adhesives introduced in the joint can increase damping drastically, but rigid loss-less adhesives can reduce damping.

Although the results presented here apply to a structural joint configuration which appears to be fairly typical of current practice, one should use extreme care in extrapolating these results to other structures. Available data are still too limited and understanding of the pertinent phenomena is still to incomplete to permit one to draw valid conclusions about the damping of joints of structures in general.

It should also be noted that the various high peaks observed in the presented damping curves are probably associated with modal shapes that favor high energy dissipation in some manner. Since such shapes are probably altered or suppressed if the joint is part of a more complicated structure, such peaks are most likely not observed in such structures. In judging the damping effectiveness of a joint which is to be incorporated in a more complicated structure from damping measurements performed on the joint by itself one should therefore probably ignore the peaks and concentrate on the overall level of damping.

F. Relation of Plate Absorption Coefficients to Loss Factors of Boundary Structures

A considerable amount of information is available concerning the loss factors of beam-like structures, whereas very little is known about absorption coefficients associated with such structures. This section therefore is concerned with some preliminary analytical steps toward obtaining interrelations between these two quantities.

1. General Expressions

From the first section of this report it is evident that the absorption coefficient γ of a portion of a plate boundary may be defined by

$$\gamma = \langle P_{diss} \rangle / \langle P_{inc} \rangle \quad , \tag{F.1}$$

where P_{inc} denotes the (length-wise) average power flow per unit length measured along the crest of a plate wave incident on the boundary. P_{diss} denotes the (length-wise) average power dissipated at the boundary, again referred to unit length measured along the incident wave crest. The brackets $\langle\ \rangle$ indicate averages taken over the angle of incidence θ, so that γ denotes the fraction of the incident power that is dissipated.

If the wave field on the plate is reverberant (i.e., independent of θ) then (ref. 4)

$$\langle P_{inc} \rangle = P_{inc} = X_p\ D\ k_p^3\ \omega \quad , \tag{F.2}$$

where X_p denotes the displacement amplitude of the plate flexural wave, k_p the wave number, ω the circular frequency, and D the flexural rigidity of the plate.

The loss factor η of a structure is defined by (ref. 2)

$$\eta = U_{diss} / 2\pi U_o \tag{F.3}$$

where U_{diss} denotes the total energy dissipated by the structure per cycle and U_o the "energy of vibration" of the structure. (For lightly damped structures U_o is essentially equal to the time-wise maximum of the total strain energy). In general η for a given structure depends on amplitude, mode shape, and frequency. No essential difficulty results if the energy terms of Eq. (F.3) are interpreted as length-wise average values rather than totals; hence such averages will be assumed henceforth. If η is now assumed to be independent of length-wise position in the structure, then

$$P_{diss} = U_{diss}\,\omega/2\pi = U_o \eta \omega \qquad (F.4)$$

and from Eq. (F.1)

$$\gamma = \langle \eta U_o \rangle / X_P^2\, k_P^3\, D \qquad (F.5)$$

2. Boundary Structures with Loss Factors Independent of Deflection Shape

For beam-like structures whose loss factors do not depend on the shapes into which they are deformed during a vibration (e.g., homogeneous viscoelastic bars or elastic bars with free viscoelastic layers), the energy losses obtained when such structures are attached to plates will be independent of the angle of incidence of plate waves, and $\langle \eta U_o \rangle = \eta \langle U_o \rangle$.

The average strain energy in a beam of flexural stiffness EI (where one might consider an "effective beam" as including a portion of the plate) may be found to be given by (ref. 4)

$$\langle U_o \rangle = \frac{EI}{4} \langle X_B^2\, (k_P \sin\theta)^4 \rangle \qquad (F.6)$$

if the beam is assumed to deflect sinusoidally (in space) with the proper spatial periodicity to conform to the incident plate waves (refs. 4, 35). From Eq. (F.3) one may then obtain

$$\gamma = \eta (EI\, k_P/4D) \cdot R \quad ; \qquad R \equiv \langle (X_B/X_P)^2 \sin^4\theta \rangle \quad . \qquad (F.7)$$

The parameter R depends on the effect of the beam on the plate motion. When the added beam is so light and soft as to have no appreciable effect on this motion, then $X_B \approx X_P$ and $R \approx 3/8$. In general, however, more detailed analyses are required. Some results directly applicable to such analyses are available (ref. 35), but the multitude of parameters complicate the analysis to such an extent that it must be considered beyond the scope of the present study.

3. Boundary Structures Attached with Viscoelastic Adhesive

In the case where structural beam is joined to a plate by a thin layer of viscoelastic glue, virtually all of the energy dissipation occurs in the viscoelastic material. One may then utilize the definition of the material's shear loss factor to write

$$U_{diss} = 2\pi\, \beta\, U_s \quad , \qquad (F.8)$$

where U_s denotes the time-wise maximum of the (length-wise average) strain energy stored in the viscoelastic layer. From Eqs. (F.1 - 4) and the foregoing one may then obtain the alternate expression

$$\gamma = \beta \langle U_s \rangle / X_p \; D \; k_p^3 \tag{F.9}$$

From an analysis similar to Kerwin's (ref. 33) one may show that for a laminate consisting of a thin viscoelastic layer between two elastic structures (i.e., a beam and plate) where these are much stiffer (in extension) than the viscoelastic layer,

$$U_s = \frac{bG}{4H} (S \; X_B \; k_p)^2 \left[\frac{\sin^3 \theta}{y + \sin^2 \theta} \right]^2 \tag{F.10}$$

if one also assumes that the wave in the laminate is sinusoidal in space and has its wavelength determined by plate waves striking the beam with angle of incidence θ. The newly introduced symbols have the following meanings:*

$$y = \frac{Gb}{H \; k_p^2} \left(\frac{1}{K_B} + \frac{1}{K_p} \right) \tag{F.11}$$

b = width
H = thickness
G = real part of complex shear modulus
} of viscoelastic layer

S = distance from neutral axis of plate to that of added beam

$K_B = E_B A_B$ = extensional stiffness of unit length of added beam

$K_p = E_p b_p h$ = extensional stiffness of unit length of strip of plate affected by beam

E_B, E_p = Young's modulus of beam, plate, material

A_B = beam cross-sectional area

h = plate thickness

b_p = effective width of plate strip

---

*The parameter y is closely related to the generalized shear parameter of Section III of Ref. 2.

4. Damping Tapes

If X_B is independent of the angle of incidence θ, then one may readily average U_s of Eq. (F.10) over θ. Introduction of this result into Eq. (F.9) then permits one to arrive at

$$\gamma = \frac{\pi}{4}\left(\frac{X_B}{X_P}\right)^2 \Gamma \psi(y) \qquad \text{(F.12a)}$$

where

$$\Gamma \equiv \frac{S^2 k_P}{D\left(\frac{1}{K_P} + \frac{1}{K_B}\right)}$$

$$\psi(y) \equiv \frac{y}{2}\left[1 - 4y + (5+4y)\left(\frac{y}{1+y}\right)^{3/2}\right] \qquad \text{(F.12b)}$$

Damping tapes represent the simplest boundary structures for which these relations apply. They are studied here not only because of their possible practical importance, but also because such a study might provide an indication of the validity of the foregoing analysis.

Figure 25 shows absorption coefficients γ measured with 2-inch wide strips of damping tape applied to an irregularly shaped aluminum plate, as well as curves obtained from calculations based on Eqs. (F.12). It is evident that theory and experiment agree quite well as long as the tape width is less than the half wavelength of a plate flexural wave, i.e., for $\lambda<4$ inches. The derivation of Eqs. (F.12) assumes that all damping is due to the length-wise deformation of the viscoelastic layer. This assumption is no longer adequate for higher frequencies where the tape width may extend over several plate wavelengths. At these frequencies one would expect to obtain additional energy dissipation due to width-wise shear deformations of the viscoelastic layer, and Eqs. (F.12) underestimate the absorption coefficient. This is also evident in the figure.

The experimental work summarized in Fig. 25 was done by methods discussed in Section I and reference 34. Commercial (Scotch Brand) damping tapes were used. The thicknesses of the adhesive layers of these tapes are a nominal 5 mils; 428B tape has 8 mil aluminum foil backing, 428C has a similar 12 mil thick backing. The adhesive properties used in the calculations were those published in reference 33. For the calculations $X_B \approx X_P$ was assumed, since the tape is much lighter and softer than the plate and may be supposed to affect the plate motion only slightly.

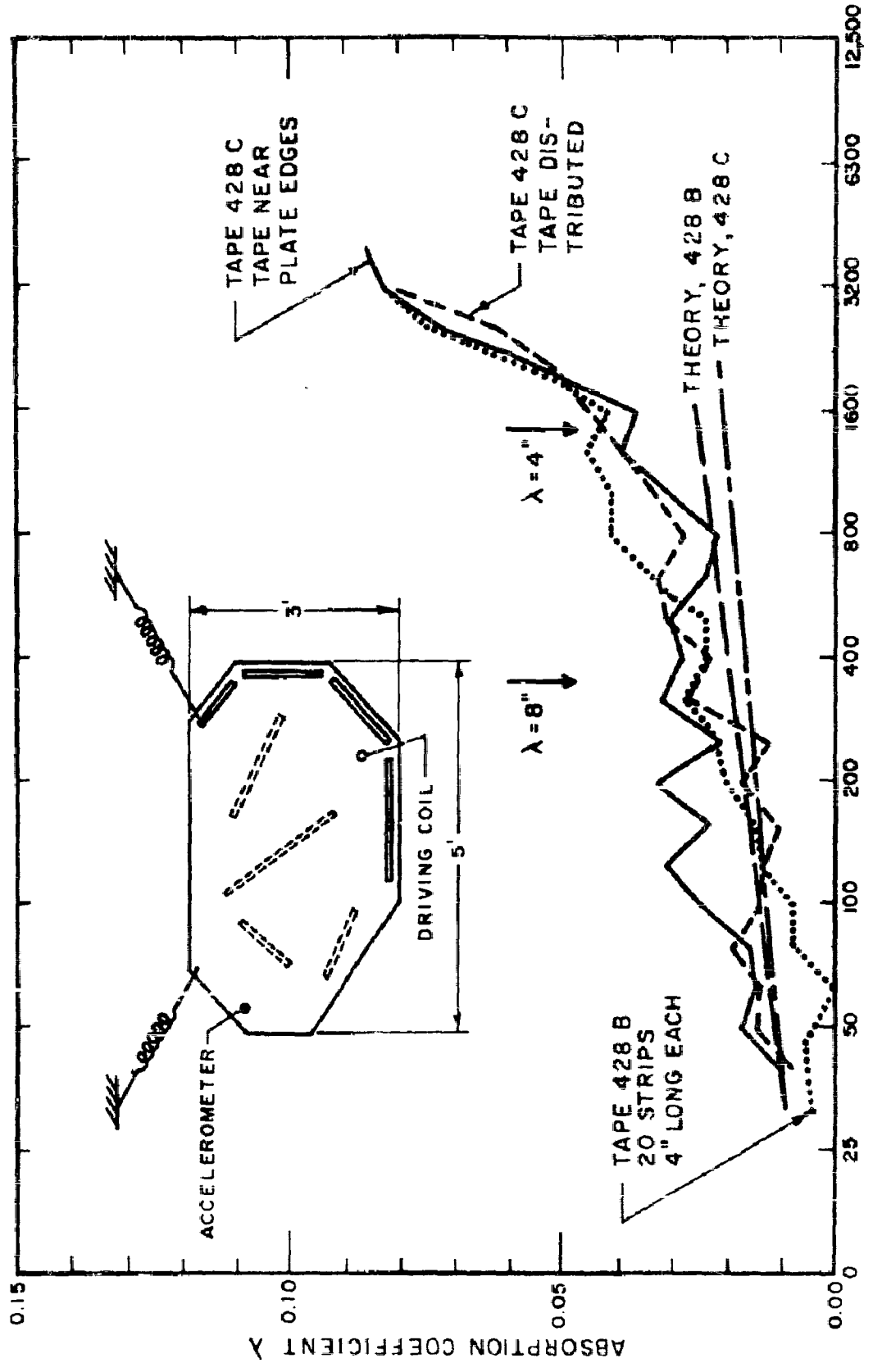

FIG.25 ABSORPTION COEFFICIENT OF MMM NO.428 DAMPING TAPE ON 1/16" THICK ALUMINUM PLATE

SECTION III

SUMMARY AND DISCUSSION

It has been shown that the responses of complex structures are strongly influenced by energy absorption at joints between substructures (measured in terms of absorption coefficients) and by the amount of coupling between an exciting sound field and the structure (described in terms of radiation resistance), in addition to the more conventional mass stiffness and damping parameters of vibration analysis.

Absorption coefficients were measured for a few structural joints, primarily to validate some of the theoretical work. Detailed studies of absorptive structures and of some of the energy dissipation mechanisms associated with them remain to be undertaken, particularly with a view toward developing configurations and design data leading to improved absorption performance.

The damping due to riveted and similar joints, which now appears to be much more significant than had previously been supposed, should merit considerable further investigation. Some of the features of joint damping brought to light by the exploratory study reported here should be explored further; their exploitation seems likely to lead to damping increases secured at little expense and weight penalty.

An introductory analytical study attempted to establish some relations between loss factors of boundary structures and the absorption coefficients realized when these structures are attached to plates. Since much loss factor data are available, whereas relatively little is known about absorption coefficients, continuation of these studies may lead to results of considerable utility.

Reductions in radiation resistance result in reduced vibrations of structures exposed to acoustic fields, hence control of these resistances constitutes an important means of vibration control. The first steps toward providing an understanding of the mechanisms responsible for radiation resistance were described in this report; extensions of these steps are being studied (ref. 17), and undoubtedly much additional investigation will be required before generally useful prediction and design procedures applicable to complex structures are developed. The ability of special beams (designed per Reference 19) to reduce radiation resistance has been demonstrated, however only by means of a laboratory experiment. Again, further studies are needed to determine if use of such structures is warranted and feasible in practice.

Detailed analytical studies of vibration absorbers utilizing viscoelastic spring elements showed these absorbers to be relatively impractical. The same conclusion was reached concerning the utility of absorbers using distributed systems.

Viscoelastic leaf springs were found to hold some promise as vibration isolation systems required to perform well over very wide frequency ranges. Their main advantages over more conventional springs lie in that they exhibit fewer transmissibility peaks and that they can be designed with frequency-variable damping. The latter is important in reducing the magnitude of the transmissibility peaks without increasing significantly the transmissibility at low frequencies. Additional study is needed to reduce these concepts to practical hard-ware.

A study of the modal behavior of beam-plate systems showed that when such systems are excited at a beam the plates adjacent to the beam may contribute significantly to reduction of the resonant beam responses. High effective beam damping is obtained when the plates are highly damped and when they are designed so that they have resonances whenever the beam has resonances.

On the other hand, beam-plate systems excited by distributed loading on the panels tend to derive only minor resonant response reduction from damping of the beams. This is so because the beams tend to couple poorly to the plates. (Plates have many more resonances than beams, hence one can not match beam resonances to each of the panel resonances.) In general, therefore, one may hope to obtain good control of beam-plate system resonant responses, no matter how the system is driven, by damping only the plates and designing these so that the resonances coincide with beam resonances.

APPENDIX I

MODAL DENSITIES

A. Plates

The natural frequencies ω_{mn} of simply supported rectangular plates are given by

$$\left(\frac{\omega_{mn}}{\pi c}\right)^2 = \left(\frac{m}{a}\right)^2 + \left(\frac{n}{b}\right)^2 \qquad (I.1)$$

where m, n are positive integers, a, b are the edge lengths, and $c = \sqrt{\omega \kappa c_L}$ is the wave velocity.*

If (m/a) and (n/b) were continuous variables, Eq. (I.1) would represent a circle of radius $(\omega/\pi c)$ in the plane of these variables, as shown in Fig. 26. However, the natural frequencies correspond only to integral values of m and n, hence to the "lattice points" indicated in the figure. The number of natural frequencies that fall below a specified value of ω thus corresponds to the number of lattice points that fall within the quarter circle of radius $\omega/\pi c$.

Actual counting of these points usually is impractical. It is more convenient to assign an area $\left(\frac{1}{a}\right)\left(\frac{1}{b}\right) = \left(\frac{1}{A}\right)$ to each lattice point (as shown in Fig. 26) and to determine how many of these lattice point areas make up the area of the quarter circle. Of course, one must make due allowance for the strips along the coordinate axes that are not associated with lattice points. One thus finds that for a simply supported plate the number of modes whose frequencies ω_{mn} are less than ω are given by

$$N_{(\omega_{mn}<\omega)} \approx \frac{1}{4\pi}\left[A\left(\frac{\omega}{c}\right)^2 - P\left(\frac{\omega}{c}\right) + \pi\right] \qquad (I.2)$$

where P = 2(a+b) denotes the plate perimeter. The modal density, obtained by differentiation of (I.2) with respect to ω, is

$$n_s(\omega) \approx \frac{1}{4\pi}\frac{A}{\kappa c_L} - \frac{P}{2\sqrt{\omega\kappa c_L}} \qquad (I.3)$$

---

*κ is the radius of gyration of the cross-section, equal to $h/\sqrt{12}$, where h represents the plate thickness. $c_L = \sqrt{E/\rho}$ is the longitudinal wave velocity in the plate material.

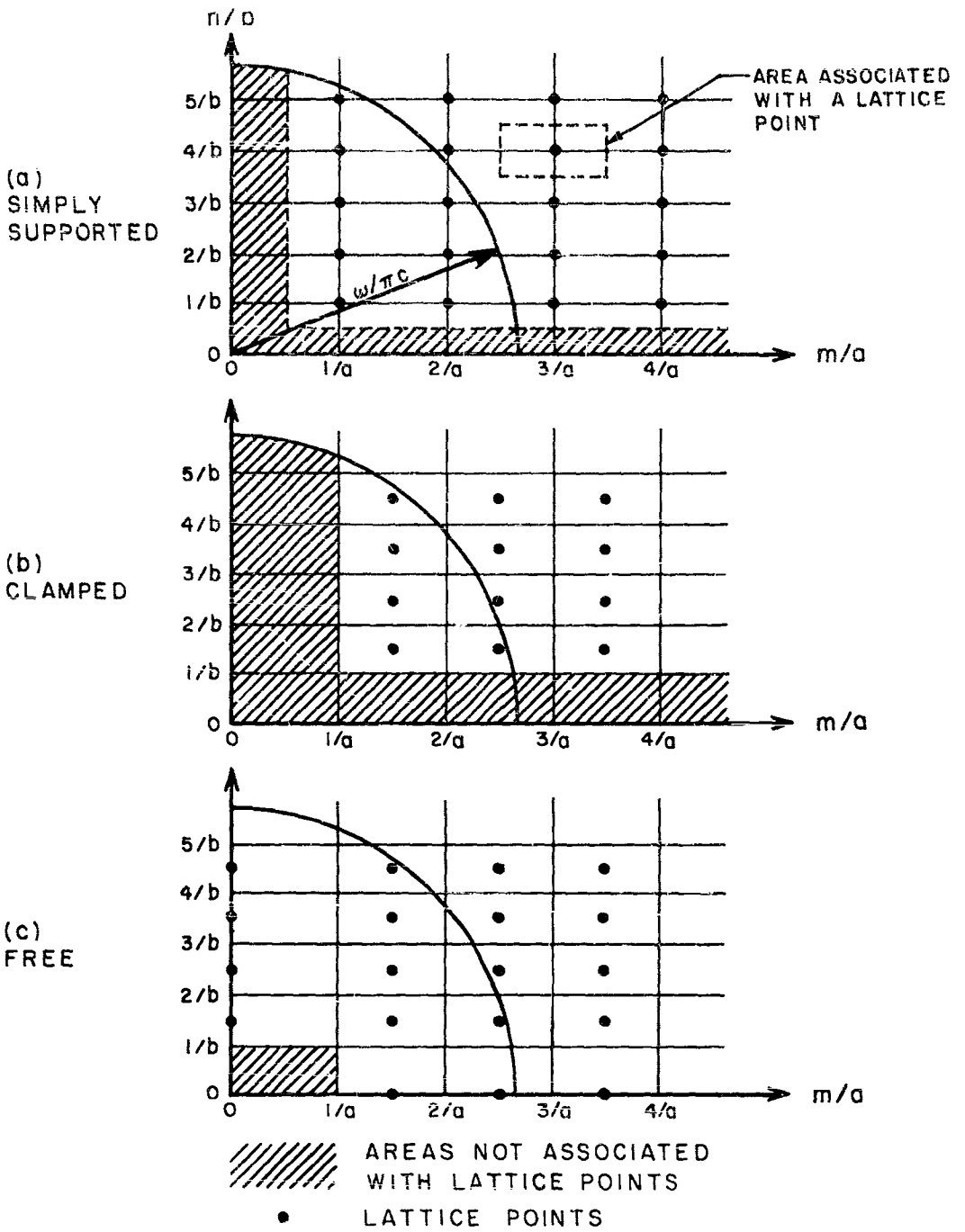

FIG. 26 MODAL LATTICES FOR RECTANGULAR PLATES

For other than simply supported boundaries the mode arrangement is not quite so easily computed, but approximations are possible. Noting that the natural frequencies of a clamped-clamped bar of length b are approximately given by $\frac{\omega_n}{\pi c} = \frac{n}{b} + \frac{1}{2b}$, $n=1,2,\cdots$, one may visualize the lattice corresponding to a plate clamped at y=0,b to be shifted upward by an amount $\frac{1}{2b}$ with respect to the lattice of Fig. 26. Similarly, clamping at x=0,a would shift the lattice to the right by an amount $\frac{1}{2a}$. If one now accounts for the areas within the quarter circle that are not associated with lattice points, one may obtain the number of modes, as before. For a fully clamped plate one finds

$$\begin{aligned} N_{(\omega_{mn}<\omega)} &\approx \frac{1}{4\pi}\left[A\left(\frac{\omega}{c}\right)^2 - 2P\left(\frac{\omega}{c}\right) + 4\pi\right] \\ n_s(\omega) &\approx \frac{1}{4\pi}\left[\frac{}{\kappa c_L} - \frac{P}{\sqrt{\omega\kappa c_L}}\right] \end{aligned} \qquad (I.4)$$

Plates with free edges may be treated similiarly. Since the natural frequencies of a bar with free-free ends are exactly the same as those of the same bar with clamped-clamped ends, the lattice for a free plate should be the same as that for a fully clamped one. However, a free plate may also deform in only one coordinate direction at a time, i.e., like a bar, so that additional lattice points occur where the lattice lines intersect the coordinate axes. For a free plate, then,

$$\begin{aligned} N_{(\omega_{mn}<\omega)} &\approx \frac{1}{4\pi}\left[A\left(\frac{\omega}{c}\right)^2 + 4\pi\right] \\ n_s(\omega) &\approx \frac{A}{4\pi\kappa c_L} \quad . \end{aligned} \qquad (I.5)$$

Note that at high frequencies one obtains the same modal density for all boundary conditions, namely

$$n_s \approx \frac{A}{4\pi\kappa c_L} \quad . \qquad (I.6)$$

This corresponds to a frequency separation between modes of

$$\Delta f = \frac{\Delta\omega}{2\pi} = \frac{1}{2\pi n_s} \approx \frac{hc_L}{A\sqrt{3}} \qquad (I.7)$$

B. Beam-Plate Systems

Consider an agglomeration of panels, frames, and stringers, as is common to aircraft construction. If the frames and stringers were infinitely rigid they would remain motionless, and the modal density would simply be the sum of the modal densities for all of the panels. Actual reinforcing structures possess some flexibility, so that adjacent panels may be expected to interact and the modes of the total structure will be complicated combinations of motions of all the sub-structures, but one may hope to obtain a rough estimate of the modal densities of such complicated structures by assuming that each panel adds its modes independently. The panels (which may be assumed clamped at all frames and stringers) thus contribute the following number of modes below the frequency ω:

$$N^P(\omega) = \frac{\omega^2}{4\pi} \sum_{i=1}^{\nu_P} \frac{A_i}{c_i^2} - \frac{\omega}{2\pi} \sum_{i=1}^{\nu_P} \frac{P_i}{c_i} + \nu_P \quad , \qquad (I.8)$$

where ν_p denotes the number of the panels. For panels of the same material and of uniform thickness, Eq. (I.8) may also be written as

$$N^P(\omega) = \frac{A}{4\pi}\left(\frac{\omega}{c}\right)^2 - \frac{B}{\pi}\left(\frac{\omega}{c}\right)^2 + \nu_P \qquad (I.9)$$

whence

$$n^P(\omega) = \frac{A}{4\pi\kappa c_L} - \frac{B}{2\pi\sqrt{\omega\kappa c_L}} \quad , \qquad (I.10)$$

where B is the total beam (or rivet-line) length. Note that each beam is counted twice as perimeter length, once for each panel it bounds, making P=2B.

[If one wishes to refine the estimate one must consider interaction of the various structural components. Among others, one may wish to add the modes due to motion of the gross structure. The motion of a multiply beam-reinforced plate at the lower frequencies is essentially that of an orthotropic plate (ref. 16), whose stiffness is generally due primarily to the beams. If this equivalent

plate is considered unsupported, one may invoke Eq. (I.5) but use a new equivalent phase velocity c_e. If this orthotropic plate has an area equal to the total structure area A, then it contributes a number of modes given by

$$N^e(\omega) = \frac{\omega^2 A}{4\pi c_e} \qquad (I.11)$$

below ω.

The number of modes below ω in the beam-plate system will be given by

$$N_S = \frac{\omega^2 A}{4\pi}\left(\frac{1}{c_e^2} + \frac{1}{c^2}\right) - \frac{\omega B}{\pi c} + \nu_P \quad . \qquad (I.12)$$

However, usually $c_e >> c$, since the reinforcing beams in practical structures generally are considerably stiffer than the panels. Thus, inclusion of the equivalent plate modes generally modifies Eq. (I.9) only slightly, and generally adds little to the quality of the estimate.]

The frequency at which the first mode occurs may be estimated by setting $N(\omega) = 1$ in Eq. (I.8). Solution of the resulting quadratic equation results in a somewhat cumbersome expression, however. One may instead wish to consider when one obtains one mode per panel on the average, i.e., when $N = \nu_p$. The corresponding frequency f_o of the "onset of modes" then is obtained from Eq. (I.8) simply as

$$f_o \approx \frac{4B^2 h c_L}{H\sqrt{3\ A}} \quad . \qquad (I.13)$$

For the simulated aircraft panel of Fig. 3 Eq. (I.10) results in a modal density value (at high frequencies) of 0.272 modes/cps, whereas experimentally a value of 0.28 was determined. Equation (I.13) predicts onset of modes (i.e., the occurrence of $N=\nu_p=15$ modes) at 170 cps for the aircraft panel, but experimentally one finds N=15 at 100 cps - a discrepancy that may to some extent be due to experimental difficulties, but most likely is due primarily to failure of the various assumptions to hold for the lower modes and frequencies.

APPENDIX II

MEASURED LOSS FACTORS OF AIRCRAFT SUBSTRUCTURES

The loss factors of some pieces of a F-105 forward structure were measured during the course of some of the previously reported studies. These results are presented here in Figures 27, and 28. Inclusion of these data was deemed desirable here because such information seems to be lacking in the literature and because it might have some bearing on the course of future damping investigations.

The data reported here were obtained by decay rate measurements, again using essentially the techniques and instruments discussed in reference 34.

The substructures to which these data pertain included no specific damping provisions. They were complicated structures, however, made up of many panels with numerous reinforcing stringers and bulkheads, and a multitude of rivets, spotwelds, and (relatively rigid) inserts of various sorts. The structures were painted for the most part.

Rough measurement of surface area and total rivet line length showed that on the basis of the relation near the top of p. 4 a mean free path length L_m of 6 inches or less would apply for flexural waves on the surface panels of these structures. For these 1/16" thick aluminum panels a 6" wavelength corresponds to about 600 cps, so that the absorption coefficient concept might reasonably be applied to these structures for somewhat higher frequencies. Unfortunately, detailed pertinent rivet line absorption coefficient data was lacking, so that further validation of the concept could not be accomplished. This validation must be deferred to a later study.

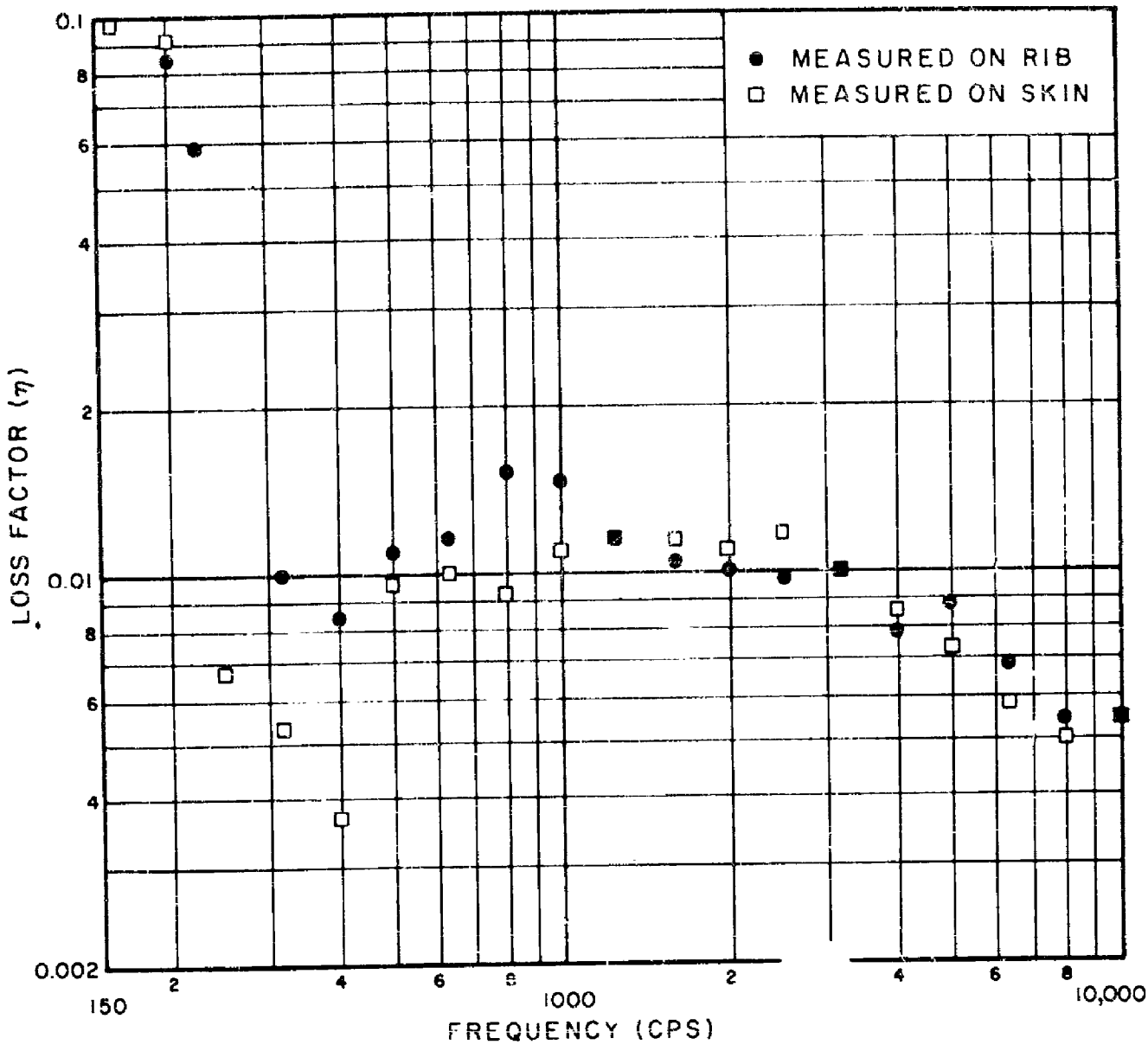

FIG. 27 LOSS FACTOR OF FRONT END CONE FROM F-105 NOSE SECTION

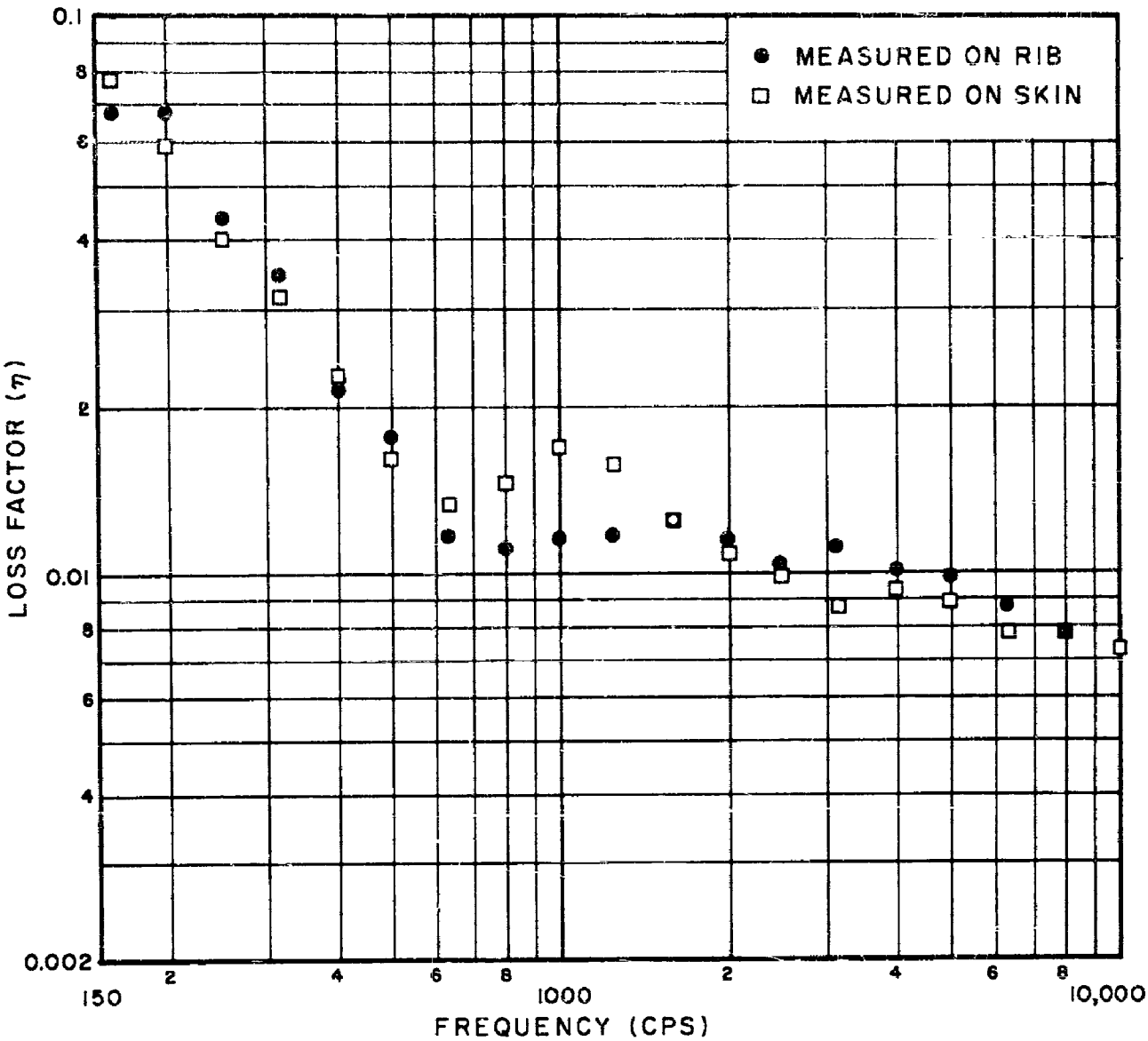

FIG. 28 LOSS FACTOR OF DOOR PANEL FROM F-105 NOSE SECTION

REFERENCE LIST

1. L. L. Beranek, Acoustics, McGraw-Hill Book Company, Inc., New York, 1954.

2. J. E. Ruzicka, Ed., Structural Damping, Amer. Soc. Mech. Engrs., New York, 1959.

3. C. W. Kosten, "The Mean Free Path in Room Acoustics", Acustica 10, 245-250 (1960).

4. L. Cremer, "The Propagation of Structure-borne Sound", (British) Department of Scientific and Industrial Research. Sponsored Research (Germany), Report No. 1, Series B, (circa 1948).

5. P. M. Morse, R. H. Bolt, "Sound Waves in Rooms", Review of Modern Physics, 16, 69-150, (April 1944).

6. R. K. Cook, "Absorption of Sound by Patches of Absorbent Materials", J. Acoust. Soc. Am. 29, (1957), 324-328.

7. M. Heckl, "Measurements of Absorption Coefficients on Plates", (to appear in J. Acoust. Soc. Am. June 1962).

8. M. Heckl, "Wave Propagation on Beam-Plate Systems", J. Acoust. Soc. Am. 33, 640-651 (May 1961).

9. R. H. Lyon and G. Maidanik, "Power Flow Between Linearly Coupled Oscillators", (to appear in J. Acoust. Soc. Am. May 1962).

10. P. W. Smith, Jr., "Estimation of Structural Response to Noise", Section III of ASD TR 61-262, Report No. 873 "Sonic Fatigue Resistance of Structural Designs" dated March 1961.

11. J. W. Miles, "On Structural Fatigue Under Random Loading", J. Aero. Sci. 21, 753-762 (1954).

12. S. H. Crandall, Ed., Random Vibration, Technology Press, Cambridge, Mass., 1958.

13. M. Heckl, "Untersuchungen über die Luftschalldämmung von Doppelwänden mit Schallbrucken", p. 1010-1014, Proc. 3rd International Congress on Acoustics, Elsevier Publishing Company, Amsterdam, 1961.

14. K. Gösele, "Schallabstrahlung von Platten die zu Biegeschwingungen angeregt sind", Acustica 3, 243-248, (1953).

15. M. Heckl, "Schallabstrahlung von Platten bei Punktförmiger Anregung", Acustica 9, 371-380 (1959).

16. M. Heckl, "Some Investigations on Grillage Vibrations", Paper U8, Acoust. Soc. Amer., 61st Annual Meeting (May 1961).

17. Contract No. NASr-47, "Research on Vibration in Complicated Structures by Energy Methods". Quarterly Status Report No. 1, October 1961.

18. H. Cramer, Mathematical Methods of Statistics, Princeton University Press, Princeton, New Jersey, 1946, Article 16.6.

19. G. Kurtze and B. W. Watters, "New Wall Design for High Transmission Loss or High Damping". J. Acoust. Soc. Am. 31, 739-748 (1959).

20. H. Oberst "Werkstoffe mit extrem hoher innerer Dämpfung" Acustica 6, Beiheft 1, pp. 144-153 (1956).

21. Lord Rayleigh, The Theory of Sound; Dover Publications, New York, 1945.

22. E. E. Ungar, "Wave Effects in Viscoelastic Leaf and Compression Spring Mounts". (Submitted for publication in Trans. ASME, Journal of Engineering for Industry.)

23. D. R. Bland, The Theory of Linear Viscoelasticity, Pergamon Press, New York, 1960.

24. e.g.; J. P. DenHartog, Mechanical Vibrations, McGraw-Hill Book Company, Inc., New York, 4th Ed., 1956, pp. 69-72.

25. A Complex Algebraic Compiler for the Royal Precision LGP-30 Digital Computer, BBN Report No. 756, 30 June 1960; submitted to BuShips, Code 345, Washington 25, D. C.

26. M. A. Harrison, A. O. Sykes, and M. Martin, "Wave Effects in Isolation Mounts". J. Acoust. Soc. Am. 24, 62-71 (1952).

27. P. M. Morse, Vibration and Sound, McGraw-Hill Book Company, Inc. New York, 1948.

28. E. E. Ungar, "Maximum Stresses in Beams and Plates Vibrating at Resonance", Series B, Trans. ASME (Journal of Engineering for Industry) 84, 149-155 (February 1962).

29. I. Dyer and M. Heckl, "Compendium of Impedance Formulas", Bolt Beranek and Newman Inc., Report No. 774 (May 1961).

30. J. H. Klumpp and L. E. Goodman, "Slip Damping of Press-Fit Joints under Linearly Varying Pressure" WADC TR 56-291 (September 1956).

31. T.H.H. Pian "Structural Damping of a Simple Built-up Beam" J. Appl. Mech. 24, 35-38 (March 1951).

32. D. J. Mead, "The Damping, Stiffness, and Fatigue Properties of Joints and Configurations Representative of Aircraft Structures", pp. 235-262 of WADC TR 59-676 "WADC - University of Minnesota Conference on Acoustical Fatigue", ed. by W. J. Trapp and D. C. Forney, Jr., (March 1961).

33. E. M. Kerwin, Jr., "Damping of Flexural Waves by a Constrained Viscoelastic Layer". J. Acoust. Soc. Am. 31, 952-962 (July 1959).

34. "Experimental Determination of Effectiveness of Vibration Damping Treatments" Bolt Beranek and Newman Inc., Report No. 755 (June 1960). Submitted to Bureau of Ships, Code 345, under Contract NObs-72452, NS 713-212.

35. E. E. Ungar, "Transmission of Plate Flexural Waves through Reinforcing Beams; Dynamic Stress Concentrations". J. Acoust. Soc. Am. 33, 633-639. (May 1961)

Aeronautical Systems Division, Air/Aeromechanics, Flight Dynamics Laboratory, Wright-Patterson AF Base, Ohio.
Rpt No. ASD-TDR-62-237, NEW APPROACHES TO FLIGHT VEHICLE STRUCTURAL VIBRATION ANALYSIS AND CONTROL. Final report, Oct 62, 76p incl illus, 35 refs. Unclassified report

New methods are outlined for dealing with the vibration responses of complex flight vehicle structures to local and to diffuse acoustic excitation. Energy absorption at structural joints and acoustic radiation resistance are shown to be important in establishing levels of these responses, and are investigated.

Viscoelastic vibration absorbers are found to-possess little practical advantage over

(over)

conventional systems. Sound-to-structure coupling is shown to be significantly reduced by the use of "Soundshear" beams. It is shown that damping of only the plates of beam-plate systems may be more desirable than damping of only the beams.

An exploratory study of the damping of aircraft structural joints, and analytical investigations of the relation between structural joint absorption coefficients and loss factors are summarized. Loss factor data pertinent to two actual aircraft substructures are appended.

1. Vibration Mechanisms
2. Damping
3. Acoustics
I. AFSC Project 1370
Task 137009
II. Contract AF33(616)-7973
III. Bolt Beranek and Newman Inc.
50 Moulton Street
Cambridge 38, Mass.
IV. Manfred A. Heckl
Richard H. Lyon
Gideon Maidanik
Eric E. Ungar
V. 903
VI. Aval fr OTS
VII. In ASTIA collection

Aeronautical Systems Division, Air/Aeromechanics, Flight Dynamics Laboratory, Wright-Patterson AF Base, Ohio.
Rpt No. ASD-TDR-62-237, NEW APPROACHES TO FLIGHT VEHICLE STRUCTURAL VIBRATION ANALYSIS AND CONTROL. Final report, Oct 62, 76p incl illus, 35 refs. Unclassified report

New methods are outlined for dealing with the vibration responses of complex flight vehicle structures to local and to diffuse acoustic excitation. Energy absorption at structural joints and acoustic radiation resistance are shown to be important in establishing levels of these responses, and are investigated.

Viscoelastic vibration absorbers are found to-possess little practical advantage over

(over)

conventional systems. Sound-to-structure coupling is shown to be significantly reduced by the use of "Soundshear" beams. It is shown that damping of only the plates of beam-plate systems may be more desirable than damping of only the beams.

An exploratory study of the damping of aircraft structural joints, and analytical investigations of the relation between structural joint absorption coefficients and loss factors are summarized. Loss factor data pertinent to two actual aircraft substructures are appended.

AF-WP-8-JUL 61 1M

1. Vibration Mechanisms
2. Damping
3. Acoustics
I. AFSC Project 1370
Task 137009
II. Contract AF33(616)-7973
III. Bolt Beranek and Newman Inc.
50 Moulton Street
Cambridge 38, Mass.
IV. Manfred A. Heckl
Richard H. Lyon
Gideon Maidanik
Eric E. Ungar
V. 903
VI. Aval fr OTS
VII. In ASTIA collection

classification

classification

Aeronautical Systems Division, Air/Aeromechanics, Flight Dynamics Laboratory, Wright-Patterson AF Base, Ohio.
Rpt No. ASD-TDR-62-237, NEW APPROACHES TO FLIGHT VEHICLE STRUCTURAL VIBRATION ANALYSIS AND CONTROL. Final report, Oct 62, 76p incl illus, 35 refs. Unclassified report

New methods are outlined for dealing with the vibration responses of complex flight vehicle structures to local and to diffuse acoustic excitation. Energy absorption at structural joints and acoustic radiation resistance are shown to be important in establishing levels of these responses, and are investigated.

Viscoelastic vibration absorbers are found to possess little practical advantage over

(over)

1. Vibration Mechanisms
2. Damping
3. Acoustics
I. AFSC Project 1370
   Task 137009
II. Contract AF33(616)-7973
III. Bolt Beranek and Newman Inc.
   50 Moulton Street
   Cambridge 38, Mass.
IV. Manfred A. Heckl
   Richard H. Lyon
   Gideon Maidanik
   Eric E. Ungar
V. 903
VI. Aval fr OTS
VII. In ASTIA collection

Aeronautical Systems Division, Air/Aeromechanics, Flight Dynamics Laboratory, Wright-Patterson AF Base, Ohio.
Rpt No. ASD-TDR-62-237, NEW APPROACHES TO FLIGHT VEHICLE STRUCTURAL VIBRATION ANALYSIS AND CONTROL. Final report, Oct 62, 76p incl illus, 35 refs. Unclassified report

New methods are outlined for dealing with the vibration responses of complex flight vehicle structures to local and to diffuse acoustic excitation. Energy absorption at structural joints and acoustic radiation resistance are shown to be important in establishing levels of these responses, and are investigated.

Viscoelastic vibration absorbers are found to possess little practical advantage over

(over)

1. Vibration Mechanisms
2. Damping
3. Acoustics
I. AFSC Project 1370
   Task 137009
II. Contract AF33(616)-7973
III. Bolt Beranek and Newman Inc.
   50 Moulton Street
   Cambridge 38, Mass.
IV. Manfred A. Heckl
   Richard H. Lyon
   Gideon Maidanik
   Eric E. Ungar
V. 903
VI. Aval fr OTS
VII. In ASTIA collection

conventional systems. Sound-to-structure coupling is shown to be significantly reduced by the use of "Soundshear" beams. It is shown that damping of only the plates of beam-plate systems may be more desirable than damping of only the beams.

An exploratory study of the damping of aircraft structural joints, and analytical investigations of the relation between structural joint absorption coefficients and loss factors are summarized. Loss factor data pertinent to two actual aircraft substructures are appended.

conventional systems. Sound-to-structure coupling is shown to be significantly reduced by the use of "Soundshear" beams. It is shown that damping of only the plates of beam-plate systems may be more desirable than damping of only the beams.

An exploratory study of the damping of aircraft structural joints, and analytical investigations of the relation between structural joint absorption coefficients and loss factors are summarized. Loss factor data pertinent to two actual aircraft substructures are appended.